

T.R.
GEBZE TECHNICAL UNIVERSITY
GRADUATE SCHOOL OF NATURAL AND APPLIED SCIENCES

**ANTIBACTERIAL AND BIOACTIVE HAP – CHITOSAN
COATINGS ON THE FUNCTIONALLY GRADED BONE-LIKE
SUBSTRATE**

ERTANCAN BABAÇ
**A THESIS SUBMITTED FOR THE DEGREE OF
MASTER OF SCIENCE**
DEPARTMENT OF MATERIALS SCIENCE AND ENGINEERING

GEBZE

2022

T.R.
GEBZE TECHNICAL UNIVERSITY
GRADUATE SCHOOL OF NATURAL AND APPLIED SCIENCES

**ANTIBACTERIAL AND BIOACTIVE HAP –
CHITOSAN COATINGS ON THE
FUNCTIONALLY GRADED BONE-LIKE
SUBSTRATE**

ERTANCAN BABAÇ

**A THESIS SUBMITTED FOR THE DEGREE OF
MASTER OF SCIENCE**

DEPARTMENT OF MATERIALS SCIENCE AND ENGINEERING

THESIS SUPERVISOR
PROF. DR. METİN USTA
II. THESIS SUPERVISOR
DR. YASEMİN TABAK

GEBZE

2022

T.C
GEBZE TEKNİK ÜNİVERSİTESİ
FEN BİLİMLERİ ENSTİTÜSÜ

FONKSİYONEL DERECELENDİRİLMİŞ
KEMİK BENZERİ YAPININ HAP –
CHITOSAN İLE BİYOAKTİF VE
ANTİBAKTERİYEL KAPLANMASI

ERTANCAN BABAÇ
YÜKSEK LİSANS TEZİ
MALZEME BİLİMİ VE MÜHENDİSLİĞİ ANABİLİM DALI

DANIŞMANI
PROF. DR. METİN USTA
II. DANIŞMANI
DR. YASEMİN TABAK

GEBZE
2022



YÜKSEK LİSANS JÜRİ ONAY FORMU

GTÜ Fen Bilimleri Enstitüsü Yönetim Kurulu'nun 03/02/2022 tarih ve 2022/06 sayılı kararıyla oluşturulan jüri tarafından 24/02/2022 tarihinde tez savunma sınavı yapılan Ertançan Babaç'ın tez çalışması Malzeme Bilimi ve Mühendisliği Anabilim Dalında YÜKSEK LİSANS tezi olarak kabul edilmiştir.

JÜRİ

ÜYE
(TEZ DANIŞMANI) : Prof. Dr. Metin USTA

ÜYE : Doc. Dr. Kemal KORKMAZ

ÜYE : Doc. Dr. Salih DURDU

ONAY

Gebze Teknik Üniversitesi Fen Bilimleri Enstitüsü Yönetim Kurulu'nun
...../...../..... tarih ve/..... sayılı kararı.

İMZA/MÜHÜR

SUMMARY

Porous silicon nitride, have been sintered and characterized with a primary purpose to develop a material to be used as bone substitute. Functionally graded materials (FGM) are preferred to represent the human bone. Tape casting provides a good grading for this type of materials. Sol-Gel coating techniques have been used at previous studies for FG Silicon Nitrides produced by tape casting.

For preparation of the slurries, there are some additions that needs to be added. The main powder and the sintering additives are the first step for preparing the slurry. Silicon nitride powders, needs high sintering temperatures which is why there is a need of sintering additives. Yttrium Oxide and Aluminum Oxide powders used for this purpose. Then the other additives are included to the solution.

After preparation of silicon nitride green bodies (including the lamination and pressing), they sintered at air at 1500°C to see the porous and dense structure. The sintering process gave us dense upper layer for the Functionally Graded silicon nitride and prepare the surface for the coatings. For this study, the main goal is to improve the bioactivity with the addition of HAp- Chitosan composite coatings.

Final samples tested for the existence of apatite layer at Simulated Body Fluid after microstructural examination and the results were evaluated. The tape casting slurries were prepared with optimum prescriptions, using rheological results for non-aqueous based solutions. As a result, bioceramic material, with bone-like microstructure has higher bioactivity, containing micro and macro pores with gradual transition has been obtained.

Anahtar Kelimeler: Silicon Nitride Ceramics, Bone-Like Structures, Dip – Coating – Bioactivity, Simulated Body Fluid.

ÖZET

Yapısı itibariyle poroz Silisyum Nitrür, mekanik özellikleri ve biyoinert yapılarından dolayı günümüzde sıkça kullanılmaktadır. Poroz yapıları nedeniyle kemik ve benzeri yapılar oluşturulmak adına literatürde üzerinde çalışılmış ve güncel olarak da çalışılmaktadır. Kemik, yapısı gereği bir inorganik ve organik kısım olmak üzere iki farklı yapıya sahiptir. Bu yapıyı yakalamak amacıyla günümüzde fonksiyonel derecelendirilmiş malzemelerin kullanım alanı olarak önemli bir alan oluşturmuştur.

Şerit döküm için gereken çamuru hazırlama aşamasında hazırlanan çözeltinin içeriği büyük önem ifade etmektedir. Bu bağlamda gereken viskozite ve reolojik değerler ölçülmeli ve gereken eklemeler yapılmalıdır. Bu bağlamda yitrium oksit ve alumina ilaveleri yapılmıştır. Daha sonrasında gereken çözücü, bağlayıcı ve dispersan ilaveleri yapıda gereken viskozite ve reolojik değerleri dengelemek, dökümü mümkün olan en iyi seviyede gerçekleştirmek için yapıya eklenmiş ve döküm işlemleri gerçekleştirilmiştir. Döküm işlemlerinden sonra, lamine edilerek preslenmiş ve ardından ısıl işlemler uygulanmıştır. Sonrasında, yapıyı mekanik açıdan geliştirmek için 1500°C’de sinterlenmiştir.

Son adımda numunelerde Hidroksiapatit sentezlenerek iç yapıya dope edilmiş ve kaplanmıştır. Sonrasında Kitozan çözeltisine daldırılarak yüzeyde bir Hap-Kitozan kaplaması oluşturulmuştur. Testlerde numuneler Yapay Vücut Sıvısı içerisinde belirli periyotlarda bekletilerek yüzeydeki apatit tabaka oluşumu ve süresi incelenmiştir. Bu işlemlerin ardından numuneler SEM, XRD, vb. karakterizasyon işlemlerine tabii tutulmuştur. Sonuç olarak biyoaktivitesi artırılmış fonksiyonel derecelendirilmiş Silisyum Nitrür malzemeleri üretilmiş olup uygun olan parametreler incelenmiş ve bulgulara eklenmiştir.

Anahtar Kelimeler: Silisyum Nitrür Seramikler, Kemik ve Benzeri Yapılar, Daldırarak Kaplama , Biyomalzemeler , Yapay Vücut Sıvısı.

ACKNOWLEDGEMENTS

I would like to thank Prof. Dr. Metin USTA, for all his guidance with his knowledge and experience in the problems I encountered on this long journey. I would like to express my respect and gratitude for providing all of his students with the work ethic that will be exemplary in all of our academic careers.

I would like to thank Dr. Yasemin TABAK, for her emotional support, protective attitudes and support at the thesis stage.

I would like to thank Research Assistant MSc Engineer Ahmet Arda İNCEYER for his valuable support and helpful approach during the thesis process.

For their technical support during my thesis phase, I would like to pay my respects to Dr. Salim Levent AKTUĞ and Specialist Ömer Faruk DENİZ.

I would like to thank the members of TÜBİTAK-MAM Biofun group for their support.

I would also like to thank Expert Cem ALİM and Researcher Deniz Kutlu TAŞKIN for their help in laboratory studies, being open to support and sharing their experience during the experimental phases.

I would like to express my deepest gratitude to my dear mother Şaziye BABAÇ and my family for their endless support, love and sacrifices at every stage of my life.

Finally, I would like to express my gratitude to Marlene Maral TUĞUTLU, who supported me endlessly at every stage of my life.

This thesis was part of “120N266- Development of Functionally Graded Silicon Nitride Materials with Improved Bioactivity” international project of TÜBİTAK MRC-Materials Institute, BioFun Group and SAS- Slovak Academy of Science of Slovakia.

TABLE of CONTENTS

	<u>Page</u>
SUMMARY	v
ÖZET	vi
ACKNOWLEDGEMENTS	vii
TABLE of CONTENTS	viii
LIST of ABBREVIATIONS and ACRONYMS	x
LIST of FIGURES	xi
LIST of TABLES	xiv
1. INTRODUCTION	1
2. BIOCERAMICS	3
3. SILICON NITRIDE CERAMICS	6
3.1. General Properties	6
3.2. Chemical Structure of Silicon Nitride	6
3.3. Phase Diagrams of Silicon Nitride	8
4. FUNCTIONALLY GRADED MATERIALS	11
5. TAPE CASTING (DOCTOR BLADE METHOD)	13
5.1. Sintering Mechanism Functionally Graded Silicon Nitride Substrates	15
6. SOL- GEL METHODS	18
6.1. Sol-Gel Coating Methods	19
6.1.1. Spin-Coating	19
6.1.2. Roll-Coating	20
6.1.3. Spray-Coating	21
6.1.4. Electrostatic Bell Coating	22
6.1.5. Dip-Coating	23
6.2. Sol-Gel Synthesis of Powders	25

6.2.1. Components Used for Sol-Gel Method	26
6.2.2. Hydroxyapatite	29
6.2.3. Chitosan	31
7. SIMULATED BODY FLUID (SBF)	33
8. EXPERIMENTAL STUDIES	35
8.1. Materials and Methods	35
8.2. Preparation of Substrates via Tape Casting	37
8.2.1. Surface Treatments	44
8.3. Synthesis of Hydroxyapatite via Dip-Coating	47
8.3.1. Preparation of the Sols	47
8.3.2. Aging of the Sols	48
8.3.3. Coating Process	48
8.3.4. Drying	49
8.3.5. Calcination	49
8.4. Coating of Chitosan via Dip-Coating	49
8.4.1. Sintering of Chitosan Coated Substrates	51
8.5. Preparation of Simulated Body Fluid (SBF)	51
9. RESULTS AND DISCUSSIONS	53
9.1. Characterization of the substrates	53
9.2. Characterization of Synthesis and Coatings of Hydroxyapatite	56
9.3. Characterization of Coatings with Chitosan	61
9.4. Bioactivity Tests using Simulated Body Fluid	65
10. CONCLUSION	70
REFERENCES	72
BIOGRAPHY	76

LIST of ABBREVIATIONS and ACRONYMS

<u>Abbreviations and Acronyms</u>	<u>Explanations</u>
α	: Alpha
β	: Beta
$^{\circ}\text{C}$: Celcius degree
cm	: Centimeter
$^{\circ}$: Degree
δ	: Delta
h	: Hour
g	: Gram
γ	: Gamma
GPa	: Giga Pascal
K	: Kelvin
kg	: Kilogram
μ	: Micron
min	: Minute
μm	: Micrometer
MPa	: Mega Pascal
W	: Watt
Al	: Aluminum
Ca	: Calcium
FGM	: Functionally Graded Material
HAp	: Hydroxyapatite
N	: Nitrogen
O	: Oxygen
P	: Phosphate
SBF	: Simulated Body Fluid
SEM	: Scanning Electron Microscope
Si	: Silisium
Ti	: Titanium
V	: Vanadium

XRD : X-Ray Diffraction
Y : Yttrium



LIST OF FIGURES

Figure No:		Page
1.1:	Illustrations of various implants and devices used to replace or enhance the function of diseased or missing tissues and organs.	1
2.1:	Examples of Si ₃ N ₄ implants for use in orthopedic surgery.	5
3.1:	Structures of hexagonal β- and α-silicon nitride. Black colored circles are silicon atoms, white circles are the nitrogen atoms.	7
3.2.:	Stick-and-ball models of the structure of α-Si ₃ N ₄ and β-Si ₃ N ₄ . Si atoms are shown yellow, N atoms are shown blue.	7
3.3:	Potential Si-N-O phase diagrams containing Si-O isobars at 1500K (pressure unit bar).	9
3.4:	Temperature-concentration division from SiO ₂ to Si ₃ N ₄ in the Si-O-N phase diagram.	10
4.1:	Structure of human bone as a functionally graded material.	11
5.1:	Principle of doctor blading using a blade for coating liquid that already feed and started moving relatively to the substrate.	13
5.2:	The required solution components for tape casting.	14
5.3:	Flow chart of production of Functionally graded materials with Tape Casting.	15
5.4:	Triple phase diagram of SiO ₂ -Y ₂ O ₃ phase relationship at 1600-1750°C.	16
6.1:	Sol-Gel coating Methods.	19
6.2:	Schematic representation of the principle of spin coating process.	20
6.3:	a) Schematic of forward roll coating (left), (b) reverse roll coating.	21
6.4:	Dip-coating stages: (a) immersion; (b) start-up; (c) deposition; (d) drainage and (e) evaporation.	23
6.5:	Some Types of Catalysts used for Sol-Gel method.	28
7.1:	The structure of hydroxyapatite crystals.	29
7.2:	Crystal Structure of Chitin and Chitosan.	31
8.1:	Glenn Mills Inc. Ball milling machine.	36
8.2:	MSE TC-0901AL Tape casting device and casting example.	37

8.3:	The tape casted films on glasses a) Bulk, b) %3 Graphite V, c) %5 Graphite V, d) %8 Graphite V.	38
8.4:	a) The Lamination and b) Cutting process.	39
8.5:	a) Preparation for Vacuuming b) After Cold Isostatic Pressing.	39
8.6:	Protherm Heat Treatment Oven.	41
8.7:	Heat treatment process (Left) and final substrate (Right).	42
8.8:	Surface of the final substrates.	43
8.9:	Reverse-Flow etching system.	44
8.10:	Preparation of the Sols at room temperature.	45
8.11:	Substrates after the coating and calcination.	47
8.12:	Preparation of Chitosan Sols at room temperature.	47
8.13:	Coating before the sintering process with different parameters.	48
8.14:	Preparation of Simulated Body Fluid.	49
8.15:	Immersion of samples in SBF.	50
9.1:	XRD analysis of UBE silicon nitride powders (Intensity vs. 2 θ degree)(a and b).	51
9.2:	BET analysis of UBE Silicon Nitride powder (Intensity vs particle size distribution).	52
9.3:	SEM Results of the Silicon Nitride powders a) x5000 b) x30000	52
9.4:	SEM images of the substrates. Images a and b shows the section without etching. Images c shows etched substrate from section. Image d shows the surface of the etched substrate.	53
9.5:	SEM images of HAp coated substrates from section. Image a and b shows unetched sections. Image c and d shows etched surface.	54
9.6:	XRD Results of unetched HAp coated substrate.	55
9.7:	XRD Results of etched HAp coated substrate.	56
9.8:	3D Mapping of Surface Roughness for unetched and uncoated substrate.	57
9.9:	3D Mapping of Surface Roughness for unetched and coated substrate.	57
9.10:	3D Mapping of Surface Roughness for etched and uncoated substrate.	58
9.11:	3D Mapping of Surface Roughness for etched and coated substrate.	58

9.12:	SEM images of HAp-Chitosan coated substrates (a and b is unetched) (c and d is etched).	59
9.13:	XRD Results of unetched substrate after chitosan dipping.	60
9.20:	SBF tests of unetched hydroxyapatite coated and hydroxyapatite/chitosan coated substrates.	
9.14:	XRD Results of etched substrate after chitosan dipping.	61
9.15:	3D Mapping of Surface Roughness unetched and chitosan coated substrate.	62
9.16:	SEM images of substrates at SBF for 24 hours. a) Without coating. b) Unetched HAp coated. c) Etched HAp coated d) HAp-Chitosan coated	63
9.17:	SEM images of substrates at SBF for 72 hours. a) Without coating. b) Unetched HAp coated. c) Etched HAp coated d) HAp-Chitosan coated	64
9.18:	SEM images of substrates at SBF for 144 hours. a) Without coating. b) Unetched HAp coated. c) Etched HAp coated d) HAp-Chitosan coated	65
9.19:	SBF tests of substrates of uncoated and etched coated substrates. a) Without coating. b) Unetched HAp coated. c) Etched HAp coated d) HAp-Chitosan coated	66

LIST OF TABLES

<u>Table No:</u>	<u>Page</u>
3.1: Mechanical Properties of Silicon Nitride Ceramics.	6
6.1: Classification of Alkoxides.	26
6.2: Ion Concentrations of SBF and Human Blood Plasma.	32
6.3: Regents for preparing SBF (pH:7.40, 1L).	32



1. INTRODUCTION

Biomaterials is basically, any type of material used to make devices or particles to replace a part or a function of the human body in a safe, reliable, economic, and physiologically acceptable manner [Mori, 1992]. Basically the materials that have a purpose to be used for biological systems called biomaterials. As the time passes by the biomaterials found themselves very large area of applications, specially for human body. Still there are a lot of research going on for developing biomaterials, for the purpose of making human life better, safer, and mostly easier.

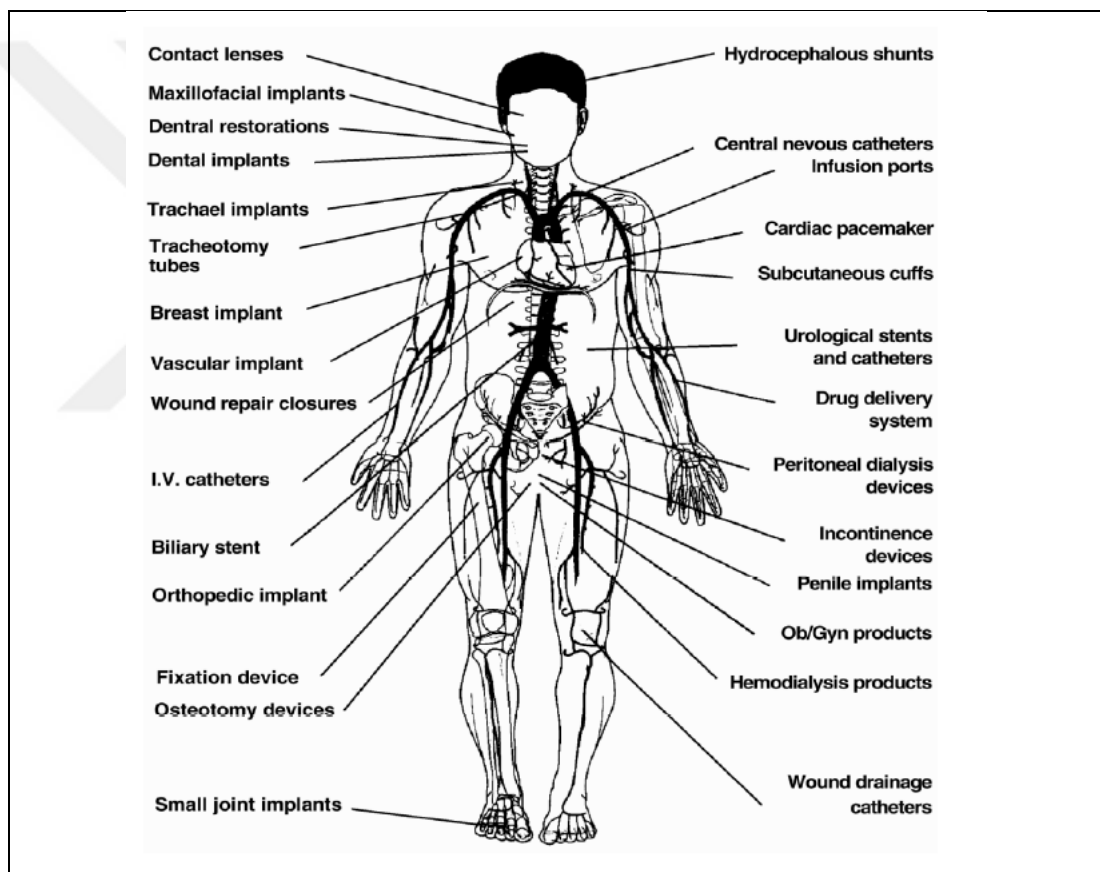


Figure 1.1: Illustrations of various implants and devices used to replace or enhance the function of diseased or missing tissues and organs.

Through the history of biomaterials metal, polymer and ceramic materials and their combinations have been used for the purpose. At the industry there are a lot of applications of metals specifically for implantation at dental or medical field. Metals such as stainless steel, cobalt-chrome alloys and titanium are used for dental implants,

hip and knee joint prostheses [Orman, 2017]. At the figure 1.1., the usage of biomaterials for human body shown and it is clearly seen that the usage area of the materials are quite different. As it is today, there are a lot of usage of Titanium and its alloys at dental industry. The development of dental implants are still a very hot topic. Not only the base materials mechanical and biological properties, the shape of the material and the surface topography of the implant also changes the bone growth mechanism. For example, the SandBlasted-Large Grit-Acid Etched surface from the Straumann Groups effect the implant industry not only because of the structure also the surface modification of the material. At this type of implants, the Ti-6Al-4V substrate has been used but the surface is sand blasted, and acid etched which in the end increase the bone growth and osseointegration.

Even though the ceramics are the oldest artificial man-made materials (Clay), they were taken into account a little later for biomedical applications [Ducheyne and Hastings, 2018]. The ceramics that has been used for biomaterials are called “bio ceramics”.

Casting slurries, containing silicon nitride powders, was poured 4 times with different pore builder additions by strip casting method, then dried, laminated on top of each other, pressed and heat treated to become the final functional graded substrate.

After the base materials are heat treated, their surfaces are first coated with hydroxyapatite synthesis by dipping method and calcined by heat treatment. Then, it was coated with chitosan once again by dip coating method and its bioactivity was investigated after the final heat treatment.

Along with the production of Functionally Graded bone-like silicon nitride materials, coating these materials is also a very difficult process. Therefore, in this thesis, FG Silicon nitride materials were first coated with dip coating method for the purpose of hydroxyapatite synthesis in order to increase bioactivity, and then coated with chitosan once again, and their effects on bioactivity were investigated.

2. BIO CERAMICS

Bioceramics are classified as bioinert, bioactive and biodegradable according to the way they interact with the host tissue. Bioactive ceramics are chemically active, thus promoting the formation of connective tissue between the bone tissue and the ceramic surface. These materials have many structural similarities with bone tissue. Used to repair and regenerate bone tissues [Naik, 2019]. The bone matrix structure consists of hydroxyapatite nanocrystals and collagen fibers. Therefore, synthetic nano hydroxyapatite (nHAp) mimics the inorganic phase of bone tissue and creates a natural environment for the bone cell osteoblast. Hydroxyapatite (HAp), tricalcium phosphate (TCP) and bioglass ceramics are widely used in bone tissue repair applications [Du et al., 2021].

Another important application of bioceramics is dental treatments. Tooth enamel is a hard, highly mineralized structure containing hydroxyapatite, a crystalline calcium phosphate. Minerals in tooth enamel are always in a natural balance, including demineralization and remineralization. Cariogenic bacteria such as *S. Mutans* on the tooth surface ferment carbohydrates and cause the formation of acid products such as lactic, acetic and propionic, which result in the dissolution (demineralization) of calcium and phosphate in the tooth enamel. This is the first step in the formation of dental caries [García-Godoy and Hicks, 2008]. Hydroxyapatite (HAp) nanocrystals are one of the agents that help remineralization. Thus, bioactive ceramics are used to support the regeneration of the mineral layer with non-invasive methods such as fissure sealants [Rao, Arathi. Neeraj, 2013]. Bioglasses are ceramics containing silica (SiO_2), calcium (CaO), phosphorus (P_2O_5) and sodium (Na_2O) that support chemical bonding between implants. The bioactivity of bioglass ceramics is based on the formation of an HAp layer that mimics bone composition [Fernandes et al., 2017].

Bioinert ceramics are passive in the microenvironment in which they are implanted. They do not enter into any reaction with the surrounding tissues and organs. Such ceramics are usually permanent implants, so they are expected to have a high potential for wear and tear for a long time after they are placed in the body. The best examples of inert bioceramics are alumina and zirconium. Alumina (Al_2O_3) has a minimal wear rate so it is often used in hip prostheses that are subject to wear and

friction. Due to its high fracture toughness, zirconium is preferred as an alternative to dental prostheses, dental implants and metal implants [Hulbert et al., 1982].

When a certain load (in the form of tension, compression or bending) is applied to the material, all materials undergo deformation under this stress. This deformation is called elastic and plastic deformation. In elastic deformation, the material returns to its original state as soon as the load (stress) is removed. In plastic deformation, when the stress condition is removed, the material cannot return to its original state and undergoes permanent deformation. During elastic deformation, atoms behave as if there is a spring between them, while in plastic deformation, the bond between atoms is broken. The deformation of the material against the stress in the elastic region gives the elasticity (young) modulus, which expresses the hardness. Thus, materials science evaluates the strength it seeks according to its intended use, according to its modulus of elasticity [Kayali et al., 1990]. The human body is made up of billions of different cell types responsible for performing specific functions. Tissues are structures where groups of similar cells come together. Considering their structural and mechanical properties, their tissues are classified as soft and hard tissues. Hard tissues such as bones and teeth have a high modulus of elasticity (young) compared to soft tissues (eg muscle tissue). The skeletal system, which includes bone tissue, is the main carrier element of the human body, therefore, its strength is high. Also, enamel is the hardest tissue in the body because it contains a lot of mineral salts and the way its crystals are arranged. Ceramic materials are brittle and inflexible because they do not undergo plastic deformation. Therefore, bioceramics are a suitable biomaterial for hard tissue replacements and dental implants rather than soft tissues [Shanmugam and Sahadevan, 2018].



Figure 2.1: Examples of Si₃N₄ implants for use in orthopedic surgery.

Biodegradable ceramics dissolve by reacting with biological fluids after a while after they are implanted in the body. These biomaterials, which are used temporarily, are biodegraded after helping the tissues to renew themselves. Bioceramics with biodegradable behavior are preferred in scaffold composites in bone tissue engineering [Naik, 2019].

Corrosion and mechanical deficiencies are among the most important problems encountered in the use of implants. The abrasion resistance of polymers is quite low compared to metals and ceramics, so they are not preferred in hard tissue treatments that are exposed to high stress. In orthopedic and dental implants, ceramics are more suitable biomaterials compared to metals for the tissue to accept the biomaterial and to perform osteogenic activity.

3. SILICON NITRIDE CERAMICS

3.1. General Properties

Silicon nitride has become a preferred ceramic in many fields due to its high temperature and abrasion resistance, thermal shock resistance, high thermal conductivity, as well as being a light material. Today, silicon nitride and its composites are used in industry such as high-performance bearings, turbine blades and spark plugs (applications requiring a material with high fracture toughness, high strength and high wear properties) [Davies, 2017], [Hampshire, 2016]. Ceramic ball bearings made of Si_3N_4 are used in industrial applications that require high strength and toughness [Supancic et al., 2009].

Table 3.1: Mechanical Properties of Silicon Nitride Ceramics.

Color	Gray
Bulk Density	3.17 g/cm ³
Hardness	1450 kg/mm ²
Compressive Strength (MPa)	>3000
Young's Modulus (GPa)	310
Poisson Rate	0.24
Thermal Conductivity	29 W/m.K

3.2. Chemical Structure of Silicon Nitride

There are three different polymorphs of silicon nitride as α , β and γ . While α and β Si_3N_4 can be produced under normal nitrogen pressure, the recently found γ polymorph requires high pressure and temperature.

The γ - Si_3N_4 structure is not included in this thesis. α and β - Si_3N_4 have trigonal and hexagonal structures, respectively, formed by corner-sharing SiN_4 tetrahedra. Both modifications consist of SiN_4 tetrahedra connected at the corners. SiN_4 tetrahedron dimensions are similar to SiO_4 . Therefore, some oxy-nitrides contain both SiN_4 and SiO_4 tetrahedra together. In the α modification, as in the β modification, each nitrogen belongs to three tetrahedra. In the β modification, there is only one layer of

SiN₄ tetrahedra structure, while α-Si₃N₄ contains two layers shifted relative to each other. This causes the c lattice parameter to double in the α-Si₃N₄ unit cell.

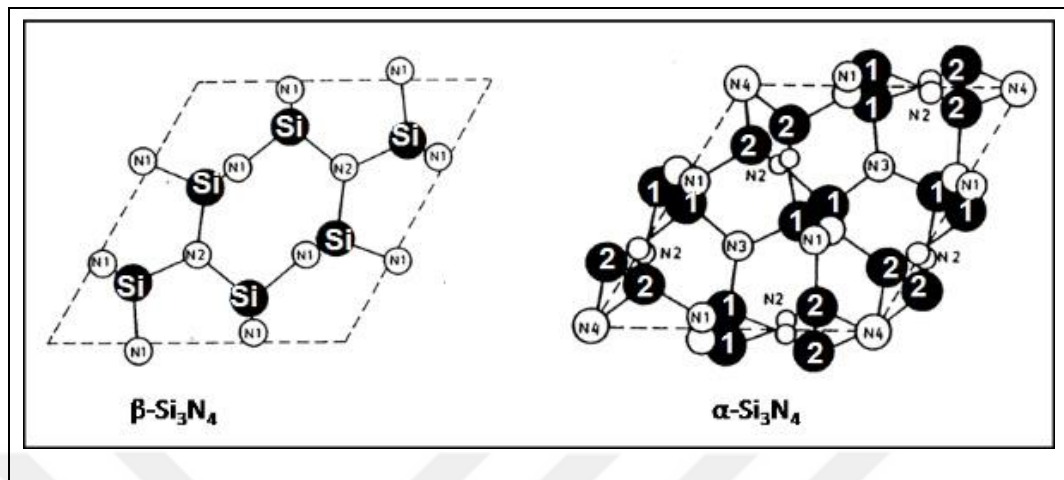


Figure 3.1: Structures of hexagonal β - and α -silicon nitride. Black colored circles are silicon atoms, white circles are the nitrogen atoms.

As shown in figures. 3.1. and 3.2., the structure shows of slightly distorted corner sharing SiN₄ tetrahedra structure distorted hexagonal circles [Somiya et al., 1991]. Hence, the double layer in α -Si₃N₄ can be thought of as a superposition of a β -Si₃N₄ layer and its counterpart inverted by 180° (Fig. 3.2).

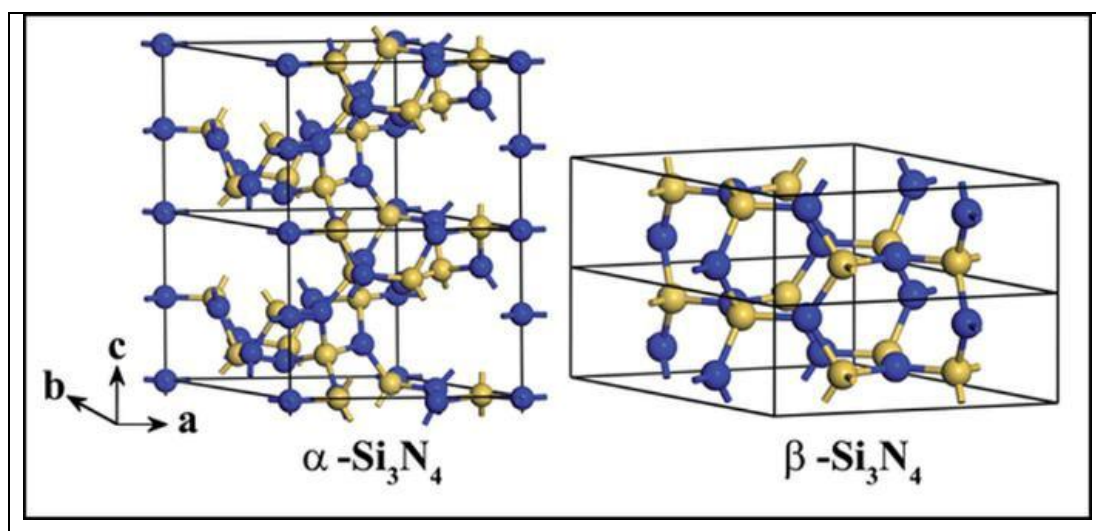


Figure 3.2: Basic model structure of α -Si₃N₄ and β -Si₃N₄. Si atoms are shown yellow, N atoms are shown blue.

3.3. Phase Diagrams of Silicon Nitride

Silicon and Silicon Nitride has high oxygen affinity so they can carry oxygen in both their solutions. In order to understand the importance of nitrogen and oxygen in the phase relations of Si₃N₄ ceramics, Si-N and Si-O binary systems are also important as well as Si-N-O triple phase diagrams (Fig. 3.3).

Silicon Nitride is a superior non-oxide ceramic that is generally preferred in high temperature and structural applications. In addition to being a very hard material, it is possible to obtain high toughness values among ceramic materials with the development of rod-like beta (beta) grains. In addition to these properties, with the understanding of its biocompatibility, the number of studies carried out in the last ten years has increased, especially in order to increase the potential for use of this material as bio ceramics. In this study, it was aimed to produce porous Si₃N₄ ceramics, which are advantageous in terms of integration with the surrounding biological tissues, by reaction bonding technique. The effects of CaO, Y₂O₃ and CeO₂ additives made to the system as sintering additions on the physical and microstructural properties of the obtained Si₃N₄ ceramics and their antibacterial behavior as a result were investigated. The results obtained show that CeO₂ is a disadvantageous sintering addition for both E. coli and S. aureus, while Y₂O₃ is the most advantageous addition. The system with the addition of CaO resulted in low bacterial growth for E. coli and high for S. aureus. Phase diagrams of systems of components can be simplified by reducing the degrees of freedom. This condition can be used where there are interconversion reactions (Eq. 3.1)



In this equation, A and B are cations and X and Y are anions. This reaction reduces the number of components to three so that two-dimensional representation of concentrations is possible [Krämer et al., 1993].

Silicon nitride ceramics are heterogeneous and multicomponent materials. They are characterized by the unique properties of α and β -Si₃N₄ polymorphs and the pronounced effect of sintering additives. The α and β modifications differ in their ability to form solid α -Si₃N₄ and β -Si₃N₄.

The formation of the microstructure depends on the quality of the Si_3N_4 starting powders, which is closely related to the chemistry of the production process, and on the other hand, the liquid phase, which provides sintering as the most important step [Jansen, 2002].

It is accepted that the phase transformation from α to β begins at about $\sim 1400\text{-}1450^\circ\text{C}$. This transformation temperature also depends on the structure of the sintered material and the composition of the additives.

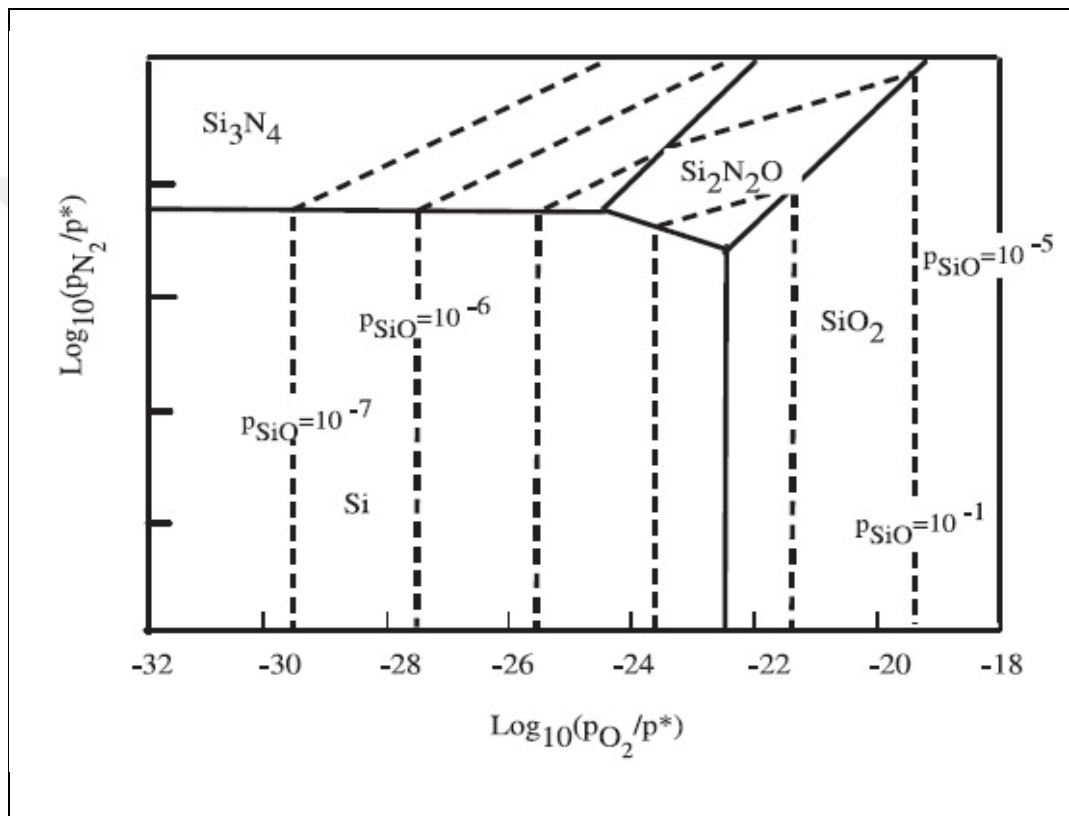


Figure 3.3: Potential Si-N-O phase diagrams containing Si-O isobars at 1500 K (pressure unit bar).

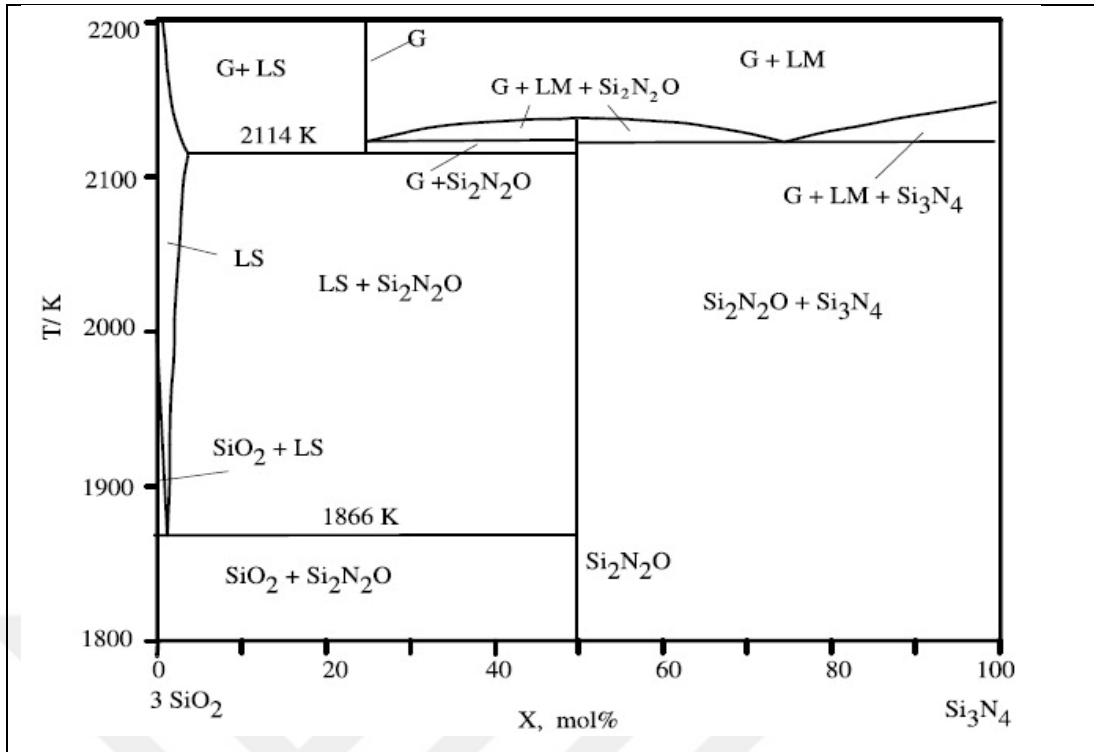


Figure 3.4: Temperature-concentration division from SiO_2 to Si_3N_4 in the Si-O-N phase diagram.

This transformation causes the transformation from α -coaxial grain to β -rod-like grain. Large phase transformation and accompanying β -grain growth provide improvements in properties such as fracture toughness and thermal conductivity of silicon nitride ceramics [Wei et al., 2001].

4. FUNCTIONALLY GRADED MATERIALS

Natural bone, due to its structure, is based on biological adaptation of functional grading. Bone architecture don't have a particularly uniform porosity. When the cross-section of the bone is examined, one part of it has a low porosity and almost dense which is called: cortical bone; and at the inner part, a high porosity structure which is called: spongy bone. It is known that porous materials surfaces can be modified with; inorganic, organic or biological coatings and inner part can be filled or doped with biocompatible and biodegradable materials or even with cells. The cells which is responsible for producing bone tissues called "osteoblasts". The minimum porous size required for osteoblasts to produce bone tissue is measured 100 μm .

The human body naturally has a highly graded structure. The figure 4.1. shows that the human bone structure is functionally naturally formed.

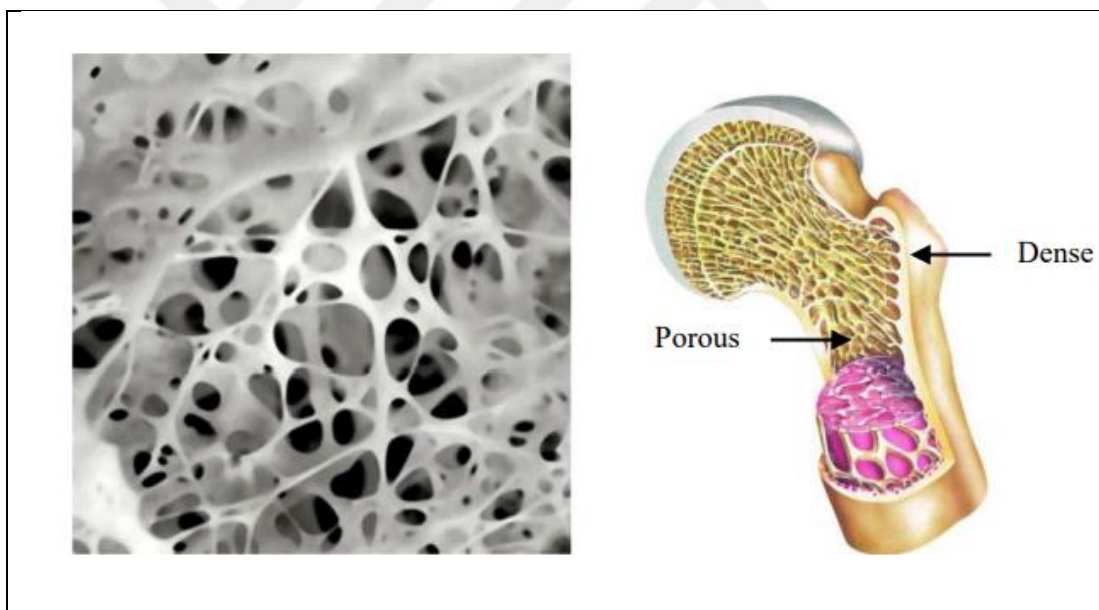


Figure 4.1: Structure of human bone as a functionally graded material.

Many natural and artificial biomedical materials, has natural functionally graded structure. In recent years, studies have focused on the weight and strength of these materials. Bio ceramics to be used as osteoimplants, to have different porous structures from the surface to inside for improvements mechanically and increased cellular structure was very hard task to be accomplished. Eventually, functionally graded materials have been produced to meet this type of materials properties.

High-density biomaterials, has problem with the stress shielding because of the elasticity modulus differences comparing to the natural bone. By adjusting the porosity ratio and shape, the porous biomaterials elasticity modulus value is close to the natural elasticity modulus value of the bone. In this way, tension at the bone-biomaterial interface formation is prevented. Also, porous biomaterials; has ability to enhance the bone-growth because of the pore size and the connection between the pores. However, the mechanical properties of this type of functionally graded materials are very weak. For these reasons, functional graded/gradient biomaterials have been developed to optimize mechanical and biological properties. Functionally Graded Materials (FGMs) can be characterized by the variation in composition and structure gradually over volume, resulting in corresponding changes in the properties of the material. This type of materials can be designed for specific applications. Various approaches based on the bulk (particulate processing), preform processing, layer processing and melt processing are used to fabricate the functionally graded materials [Dwivedi et al., 2006].

Production of functionally graded materials are more difficult than the biomaterials which has uniform and homogenous porosity. The most cost-efficient way to produce this type of materials is tape casting method. With tape casting; wide surface area, multi-layered and high quality materials can be easily produced.

5. TAPE CASTING (DOCTOR BLADE METHOD)

Tape casting is a technique that has been used in industry for large-scale fabrication of ceramic structures and lately for the multi-layered materials [Bal et al., 2006].

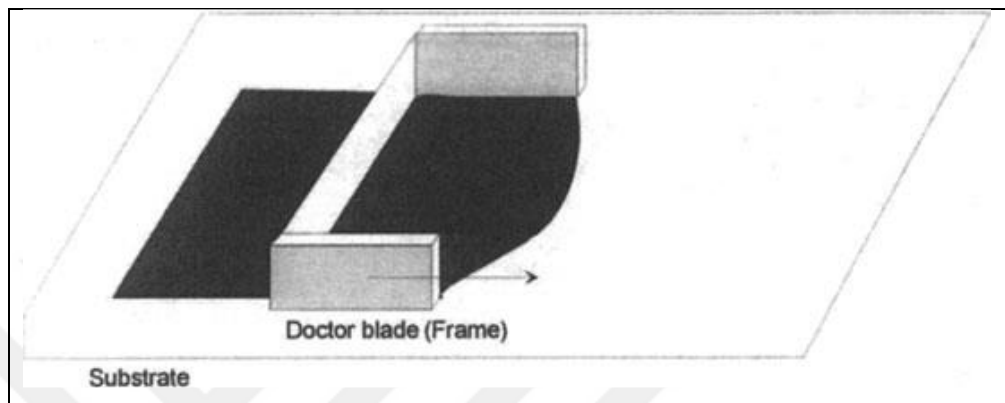


Figure 5.1: Principle of doctor blading using a blade for coating liquid that already feed and started moving relatively to the substrate.

For the preparation of the slurries which is required for tape casting method, there are some additions that need to be added. The main powder and the sintering additives are the first step for preparing the slurry. Silicon nitride powders as our main ingredient, need very high sintering temperatures which is why there is a need of sintering additives. For the sintering additions, the rare-earth oxide additives are used as the ideal additives for Silicon Nitride ceramics because they control the $\alpha \rightarrow \beta$ phase transformation rates of the ceramic, the grain growth anisotropy and the aspect ratio of the β -Silicon Nitride [Koshino et al., 2002], [Lewis et al., 2010]. Many Silicon Nitride ceramics are sintered with an additive consisting of a combination of Y_2O_3 and Al_2O_3 [Tsukamoto et al., 2006]. On cooling, the liquid phase crystallizes to an yttrium-aluminum garnet phase. The fabricated Si_3N_4 shows improved high temperature creep resistance as well as better oxidation resistance compared to the material fabricated with Y_2O_3 alone as the additive [Mazzocchi & Bellosi, 2008]. Apart from sintering additives, the other additions are included to the solutions which are solvent, dispersants, binders, and pore makers if required. After the solution is prepared and mixed, the tapes are casted at required thickness and pore amounts to have more than one type of layer.

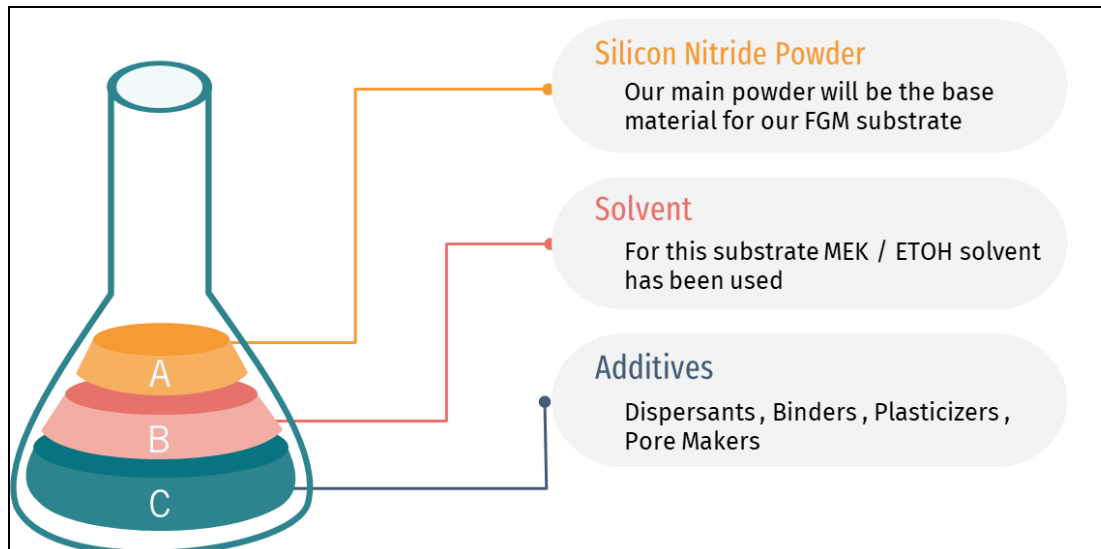


Figure 5.2: The required solution components for tape casting.

Once the Tape casting process is completed, the green bodies are needed to be laminated and pressed before sintering in order to have the required graded structure. This process is very important for the development of functionally graded materials.

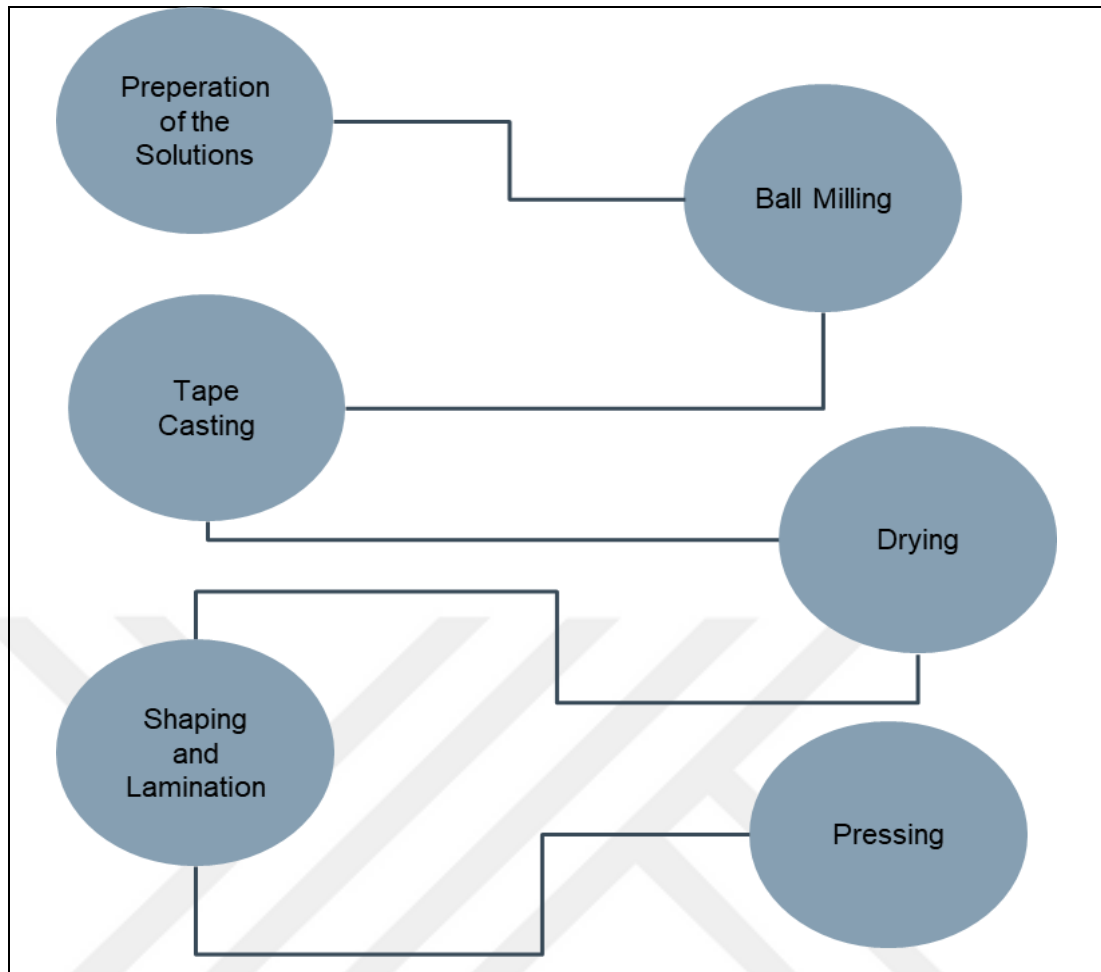


Figure 5.3: Flow chart of production of Functionally graded materials with Tape Casting.

5.1. Sintering Mechanism Functionally Graded Silicon Nitride Substrates

Sintering of silicon nitride materials are very difficult process and requires a high temperatures. Sintering additives have to be added to form a liquid and lower the required high temperatures also enhances the densification. The additives reduce the sintering temperature and make it possible to densify the material without dissociation. For sintering process to be homogenous the sintering additives must be mixed before the substrate is prepared. When starting from silicon and then nitrificate other additives can be added to the silicon powder or be infiltrated into the porous structure.

The most used method for sintering is at atmospheric pressure. It is the most cost-efficient one but requires the use of sintering additives and high temperatures. A

slight overpressure of nitrogen is always necessary. Generally rather large amounts of additives are still needed in this process.

Due to the strong covalent bond of silicon nitride, using the traditional powder technology or traditional ceramic sintering methods are difficult to sinter at high density and purity. During sintering, because of the oxide additives, a has liquid phase with low eutectic temperature which silicon nitride is prohibited to dissolve is occurring. Therefore, different additives and different compositions is being tested. Uniform distribution of these additives as finer particles and very important to be able to surround the silicon nitride grains is the motto for this additions [Ayas, 2009], [Somiya et al., 1991], [Bressiani et al., 1999].

In the three-phase diagram of the $\text{Si}_3\text{N}_4\text{-SiO}_2\text{-Y}_2\text{O}_3$ phase relationship at 1600-1750°C (Figure 5.4.) the crystalline phase is Y_2O_3 . As a crystalline phase at grain boundaries when Y_2O_3 is used. In addition to Si_3N_4 , $\text{Y}_2\text{Si}_3\text{O}_3\text{N}_4$ ($\text{Si}_3\text{N}_4\cdot\text{Y}_2\text{O}_3$) is formed. YSiO_2N as third phase A liquid phase with similar composition is formed. This liquid for sintering phase is required.

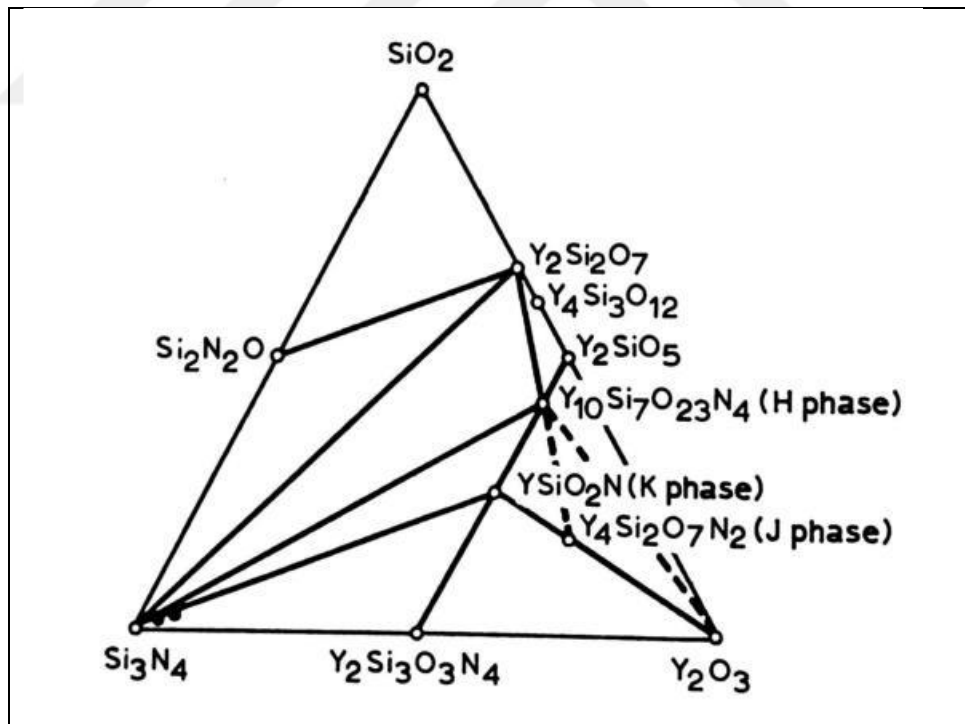


Figure 5.4: Triple phase diagram of $\text{SiO}_2\text{-Y}_2\text{O}_3$ phase relationship at 1600-1750°C.

The eutectic temperature line for the $\text{Si}_3\text{N}_4\text{-Y}_2\text{O}_3\text{-SiO}_2$ ternary system is at 1550°C . With this However, the eutectic temperature is lower due to the Al_2O_3 content of the starting powder. Depending on the increasing temperature, decomposition-precipitation may occur. The conversion from α to $\beta\text{-Si}_3\text{N}_4$ phase is completed at approximately 1650°C .



6. SOL- GEL METHODS

Sol-gel method is very important method for; providing homogeneous mixture at molecular size, reaction kinetics can be controlled, it is done at low temperature, it does not require vacuum and provides homogeneous coating of complex shaped substrates. Since high temperature is not applied, the properties of the substrate prevent phase changes and mechanical distortions that may adversely affect will be passed.

In this method, the starting chemicals are dissolved in suitable solvents, while the hydrolysis and condensation reactions occur in the sol. After the reactions mentioned, the colloidal suspension or sol is obtained. Then colloidal nanoparticles in suspension and sol form a three-dimensional network in liquid. This is called gelation. Gelation can be initiated in many ways [Chai & Ben-Nissan, 1999]. Then, depending on the final material to be obtained, different transactions are made. If powder is desired, after the gelation stage, the drying at oven atmosphere and sintering are carried out in the environment. By applying special drying conditions aerogel and xerogel can be produced. For coatings to be done, sol can be deposited on to substrate using various methods. Then drying and calcination process is done.

There are multiple coating methods in the Sol-Gel coating method. All these processes are based on the same principles. It is about dipping previously prepared sol, waiting, and then drying the substrate material that is desired to be coated on a substrate.

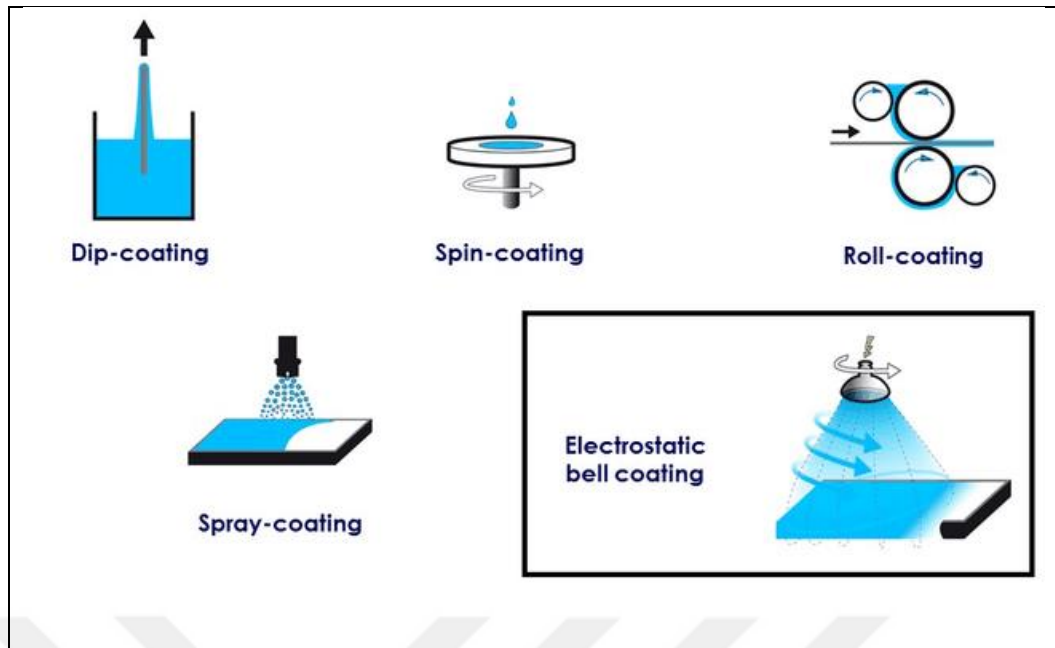


Figure 6.1: Sol-Gel coating methods.

6.1. Sol-Gel Coating Methods

6.1.1. Spin-Coating

Spin coating is a method used to coat thin films on flat surfaces. A small amount of material is applied in the middle of the layer to be coated and applied by rotating at the desired speeds for the specified time period. The devices used for this process are called spin coaters or simply spinners. The coating material applied in this coating method is usually volatile and evaporates simultaneously during the process. The thickness of the film also depends on parameters such as solution and solvent viscosity, concentration and surface tension. Looking at the mathematical modeling of the spin coating method, one of the most important factors here is the spin speed. The velocity (rpm) of the surface to be coated affects the degree of radial (centrifugal) force applied to the coating fluid, as well as the characteristic turbulence and velocity of the air. There is an inverse relationship between the coating thickness and the speed. The higher the bending angular speed, the thinner the film layer [Makhlouf, 2011]. The spin coating process has been shown in Figure 6.2.

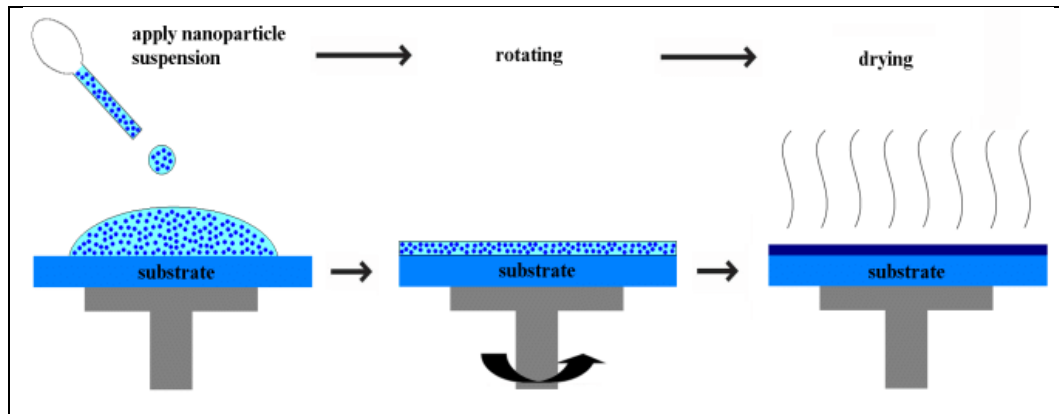


Figure 6.2: Schematic representation of the principle of spin coating process.

6.1.2. Roll-Coating

Roll coating is a process that uses three rollers to apply a coating to a flat substrate: a soft application roll, a highly polished steel roll, and a metering (or doctor) roll. Firstly, the substrate travels between the soft application roll and the steel roll. The application roll picks up the coating as it rotates, and subsequently transfers the coating to the flat sheet of metal as it passes through [Abbott Nj et al., 1972], [Alonso et al., 2003], [Greer, 1995]. Varying substrate thickness does not result in uneven coating thickness [Glawe et al., 2003].

The most simple roll-coating setup has a single rotating roller. The bottom half of the roller is dipped in a coating liquid bath as known as sol and the upper part of the roller is in contact with the substrate (Fig. 6.3). While its rotation, the coating sols forms a film on the roller's surface and rest of the sol is carried from the roller surface to a coated substrate. The amount of coating on the substrate is determined by hydrodynamics [Wright, 1994]. The rotation speed of the roller, the substrate speed, and rheological properties of coating fluid (surface tension, viscosity, and density) are factors determining coating thickness [Shim, 2013].

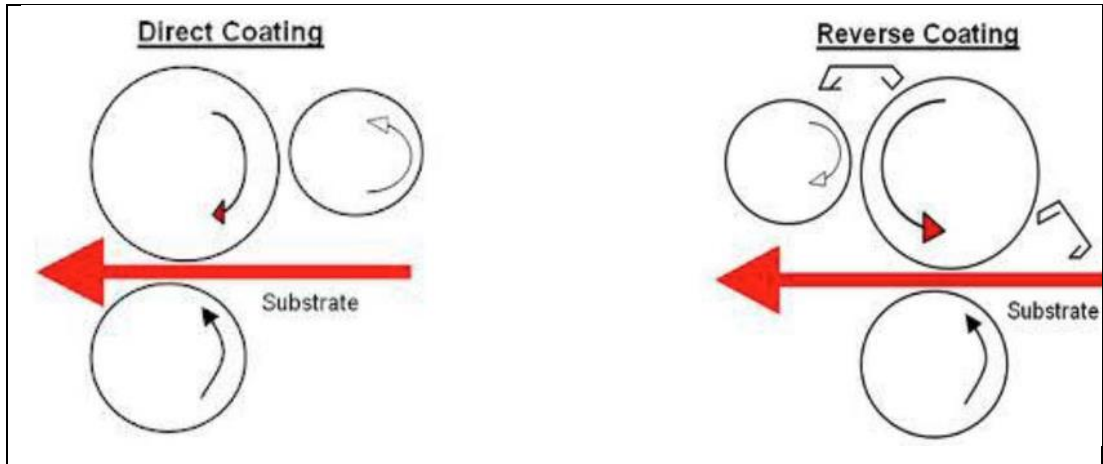


Fig 6.3: a) Schematic of forward roll coating (left), (b) reverse roll coating.

6.1.3. Spray-Coating

Spray coating techniques are widely used in industry for quite some time. The preparation of optical coatings by spray technique offers many advantages compared to the other sol-gel coating techniques, since it is realized processing speed is a lot faster, the waste of coating sols is much smaller, coating with rather short lives can be used and the coating step is suitable for establishing an continued process. The spray-coating process can be seen from Figure 6.4.

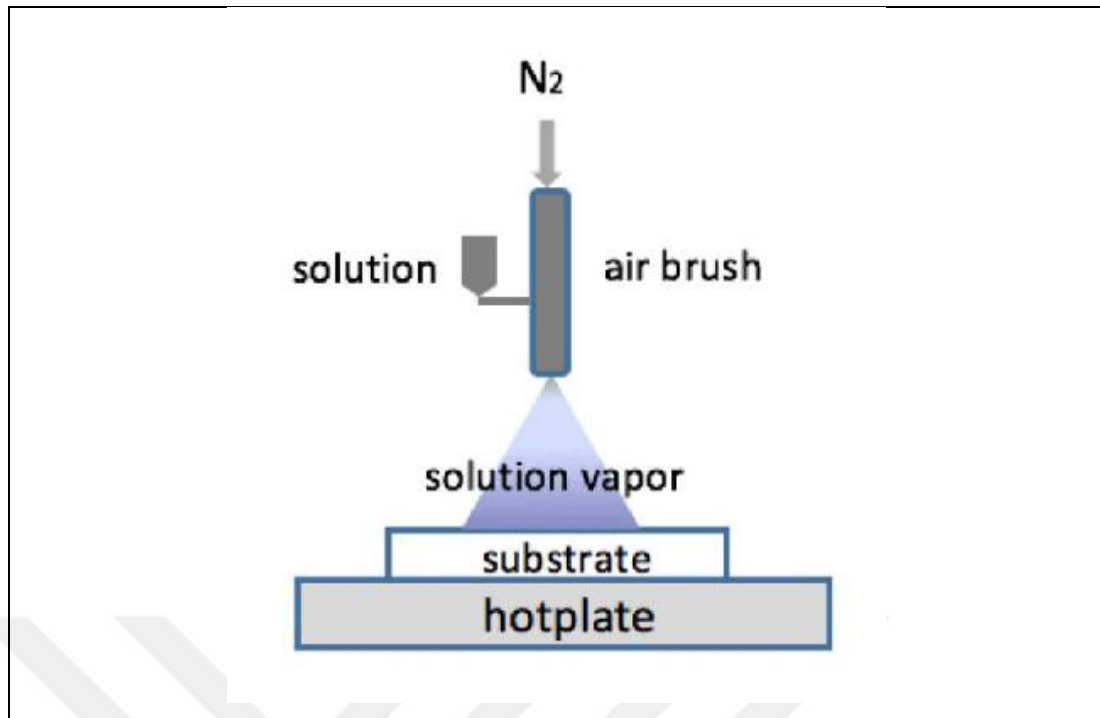


Fig 6.4: A schematic diagram of the spray coating technique.

6.1.4. Electrostatic Bell Coating

Electrostatic spraying (E-spraying) refers to the use of an electric field to assist in the spraying of liquid droplets onto a grounded substrate. The droplets in the spray are charged as they exit the spray nozzle and are attracted to the grounded substrate. By providing this electric potential difference, the driving force of droplets is accentuated, thereby increasing the transfer efficiency of the spray. Spray is a surface treatment method that sprays plastic powders onto parts. Spray is the electrostatic powder coating that we wanted to paint in the early 1980s, since the international acceptance of a more common metal surface treatment of decorative technology, generally in the early 1980s. Technology, compared with ordinary paint surface treatment, embodied advantages of advanced technology, energy efficient, safe, reliable, beautiful color and so on. The process which can be seen from Figure 6.5. Therefore, it is often used for light industry, home improvement. The working principle makes the plastic powder charged by high voltage electrostatic equipment, the coating is sprayed on the surface of the workpiece under the action of an electric field; The powder is coated in powder form by being homogeneously adsorbed on the surface of the workpiece and the powder coating passes (Fig. 6.5.).

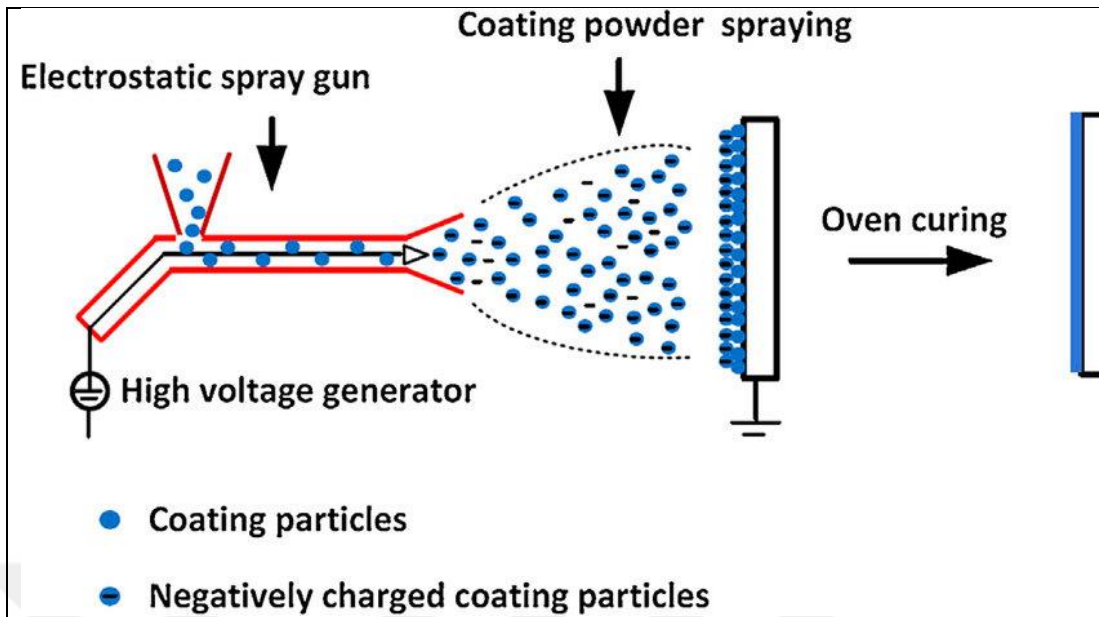


Figure 6.5: Schematic figure for Electrostatic Powder Coating.

6.1.5. Dip-Coating

It is one of the most important methods of sol-gel coating. The prepared sole of the substrate is specific. It is based on the principle of being immersed at one speed and being removed at the same speed. The dip coating method takes place in five stages: dipping, pulling up, coating, infiltration and evaporation. Usually, after drying in a water atmosphere, the film needs hardening/chemical transformation by heat treatment. The dip-coating method is graphically presented in Figure 6.6.

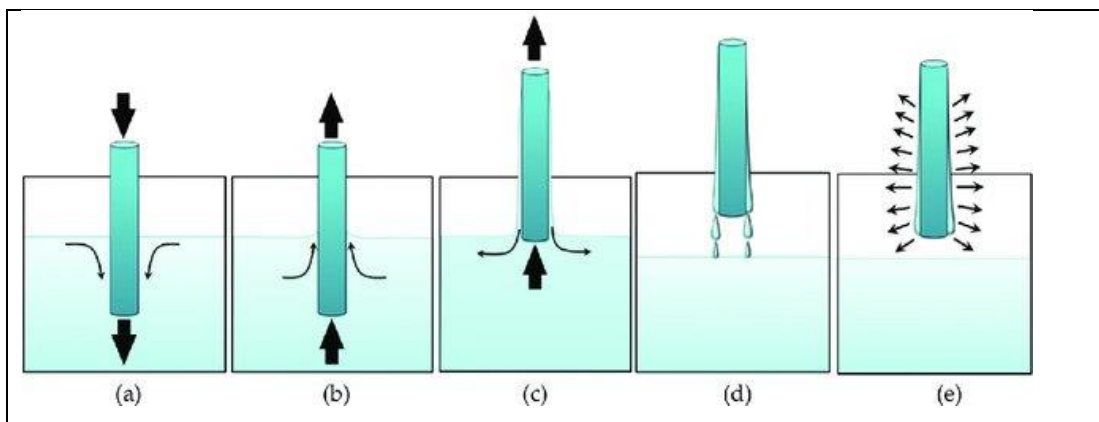


Figure 6.6: Dip-coating stages: (a) immersion; (b) start-up; (c) deposition; (d) drainage and (e) evaporation.

The thickness of the coatings made by the dip coating method; depends on the viscosity of the sol, shrinkage rate, solvent evaporation rate, shrinkage of the gel, and the environment during extrusion is a function of the conditions (temperature, pressure). To predict the thickness of the gel film The Landau-Levich relation can be used [Pillar-Little et al., 2015].

$$h = 0,94 (\eta U)^{2/3} / \gamma LV^{1/6} (\rho g)^{1/2} \quad (6.1)$$

h: Film thickness, η : Sol viscosity, U: Shrinkage velocity, γLV : Liquid-vapor surface tension, ρ : Sol-specific gravity, g: Gravitational constant [Pillar-Little et al., 2015].

6.1.5.1. Quality of the Coating

There are some properties that must be provided in the coatings applied to the implants. Pores are necessary for; transmission of fluids and nutrients, oxygen diffusion, protein absorption, which benefits at bone cell formation and attachment.) in their study they have stated,

when the pore size is larger than 100 μm , the bone permeability and facilitated cell proliferation is increased [Buyuksagis et al., 2017], stated in his study that, when the coating surface is inhomogeneous it has improved osteointegration.

Control of surface morphology of coatings; can be done with parameters like; different starting chemicals use, final heat treatment temperature and chemical additions. Roughening the surface and adding a different oxide increases the adhesion strength [Feng et al., 2003].

However, in some cases, the surface roughness at surfaces, may change with different levels may differ during dip coating and thicknesses and cracks occur in areas where the coating thickness is high [Montenero et al., 2000]. Surface roughness of the number of films coated layer also depends on the sol viscosity [Owens et al., 2016]. Adhesion with chemical bonding and no residual thermal stresses positively affects the strength [Feng et al., 2003]. Wetting is another important issue that affects the coating quality. It is a complex function dependent on sol and substrate chemistry and affects the quality of the coating. Considering the charge balance between the sol

particles and the substrate surface application can improve wetting behavior [Butts et al., 1988].

Thermal expansion coefficients of substrate and coating in sol-gel deposition technique, where they differ from each other; during heating and cooling, substrate and coating, there is a different amount of expansion and contraction occur. The residual stress causes it to occur. The crystal structure difference between the substrate and the coating is structural is another reason for incompatibility [Carrado et al., 2011]. Heat treatment temperatures and regimes are also important in terms of coating quality. Drying and calcination temperatures and regimes are determined according to the desired final product properties. For example, if thick and dense coatings are desired, high calcination temperature is required to remove residual carbon [Jiang et al., 1998].

6.2. Sol-Gel Synthesis of Powders

The sol-gel process is carried out in a suitable solvent such as ethanol, with a catalyst or without catalyst. In the presence of a catalyst, a metal-organic pre-initiator such as tetra n-butyl titanate is hydrolysis and includes condensation. The synthesis of solid materials by the sol-gel method is mostly includes wet chemistry reactions. But in general, sol-gel chemistry is based on, hydrolysis and transformation of molecular pre-initiators in the oxide network by condensation reactions. Alkoxide groups in alcohol-water solution, acidic or basic catalyst is gradually removed by hydrolysis in the presence of replaced by hydroxyl groups. gelation to form a network covering the entire solution volume It is formed by the assembly of growing polymer networks. At this gelling point, both the viscosity and the elastic modulus gradually increase. The gel is then used to form the xerogel; can be dried by evaporation, or by supercritical fluid extraction to obtain aerogel [Aurobind et al., 2006], [Livage et al., 1998], [Sobolev & Lisoivan, 1969].

Sol-gel method is a method that can be applied well in laboratory conditions and this method use is also increasing for large-scale production [P.C., 1998].

The sol-gel method generally consists of the following basic steps:

- i)* Hydrolysis of the pre-initiator
- ii)* Alcohol or water condensation of sol-gel active species

- iii) Gelation
- iv) Aging
- v) Drying
- vi) High temperature operation

The general chemical reactions involved in the sol-gel process are of great importance as they allow control in the whole process from the starting material to the final material for proper design and production of the stable phase.

6.2.1. Components Used for Sol-Gel Method

The sol-gel process involves the transition of the sol composition from a liquid “sol” phase to a solid “gel” phase [R. Gupta and Chaudhury, 2007]. Inorganic sols and gels are usually synthesized from dissolved chemical reactants in a liquid medium. Reactant containing a metal (M) in an inorganic sol or gel, is called a chemical pre-initiator. The chemical transformation of this structure is quite complex. The conversion of sol to gel likewise involves very complex reactions at the molecular level. Its reactions involve the controlled dispersion of dense colloidal particles in the sol or their gel. They also provide control of agglomeration precursors [P.C., 1998]. All soluble pre-initiators are used in the sol-gel process. These fall under two main groups. They can be identified: Metal salts and alkoxides [Bezzi et al., 2003], [Butts et al., 1988], [P.C., 1998].

- Metal Salts

The general formula of metal salts is M_mX_n . Here M is metal, X is an anionic group, m and n are also stoichiometric constants. An example of metal salts is $AlCl_3$ [P.C., 1998].

- Metal Alkoxides

Alkoxides are known by the general formula $M(OR)_n$. [Asri et al., 2016], [Stankevičiute et al., 2013]. Metal alkoxides react to reactions because of their highly electronegative OR group they contain [P.C., 1998].

Table 6.1: Classification of Alkoxides.

Alcohol R(OH)	Alkoxite	“OR” abbreviation
Methanole (CH ₃ OH)	Methoxite	OMe
Etanol (C ₂ H ₅ OH)	Ethoxide	OEt
1, propanol (n- propanol) C ₃ H ₇ OH 2, propanol(iso-propanol) C ₃ H ₇ OH	1-propoxite (n- propoxate) 2-propoxite(iso-propoxate)	OPr ^l OPr ^s
1, buthanole (n-buthanole) C ₄ H ₉ OH 2, buthanole C ₄ H ₉ OH 2, metil propanole (iso- buthanole) C ₄ H ₉ OH 2, metil- prop,2,ol (tetrao- buthanole) C ₄ H ₉ (OH)	1 butoxide (n- butoxide) 2 butoxide (sec- butoxide) 2, methyl propoxite (iso- buthoxite) Tetrao butoxide	OBu ⁿ OBu ^s OBu ⁱ OBu ^t

6.2.1.1. Solvents

Since the solution chemistry of metal salts and metal alkoxides is quite different, the pre-initiator the choice of solvent should be made according to the type of solvent. The solvent may be water or an organic solvent. Since alkoxide and water do not mix with each other, it is necessary for the reactions to take place in the sol-gel process. A suitable solvent is needed. Water as solvent for metal salts, for metal alkoxides alcohols are used. Such as CH₃OH (methanol), C₂H₅OH (ethanol), C₃H₃OH (propanol), C₄H₉OH (butanol) Alcohols are used as starting materials in the sol-gel method and are combined with metal oxides. they react.

Separately from alcohols, water has a significant effect on the sol-gel process. is evaluated. Water forms the molecular structure compared to other parameters (temperature, catalyst, etc.). and is a component that is directly involved in chemical reactions. The importance of water in the sol-gel process can be slowed down by

giving less water than shows [Kloskowski et al., 2010], [Livage and Ganguli, 2001], [Locher et al., 2005], [P.C., 1998]. In the sol-gel process, the amount of water is expressed in terms of the water/alkoxy ratio [Locher et al., 2005].

6.2.1.2. Catalysts

Catalysts used in the sol-gel method are divided into acid and base. Generally some catalysts used are presented in figure below. Catalysts are substances that increase the reaction rate by reducing the activation energy in a chemical reaction and do not undergo a chemical change when the reaction is complete. Catalysis is the name given to this change in the reaction. In a chemical reaction, the catalyst is both the reactant and the product. The catalyst provides a change in the reaction rate with lower energy expenditure in a chemical reaction.

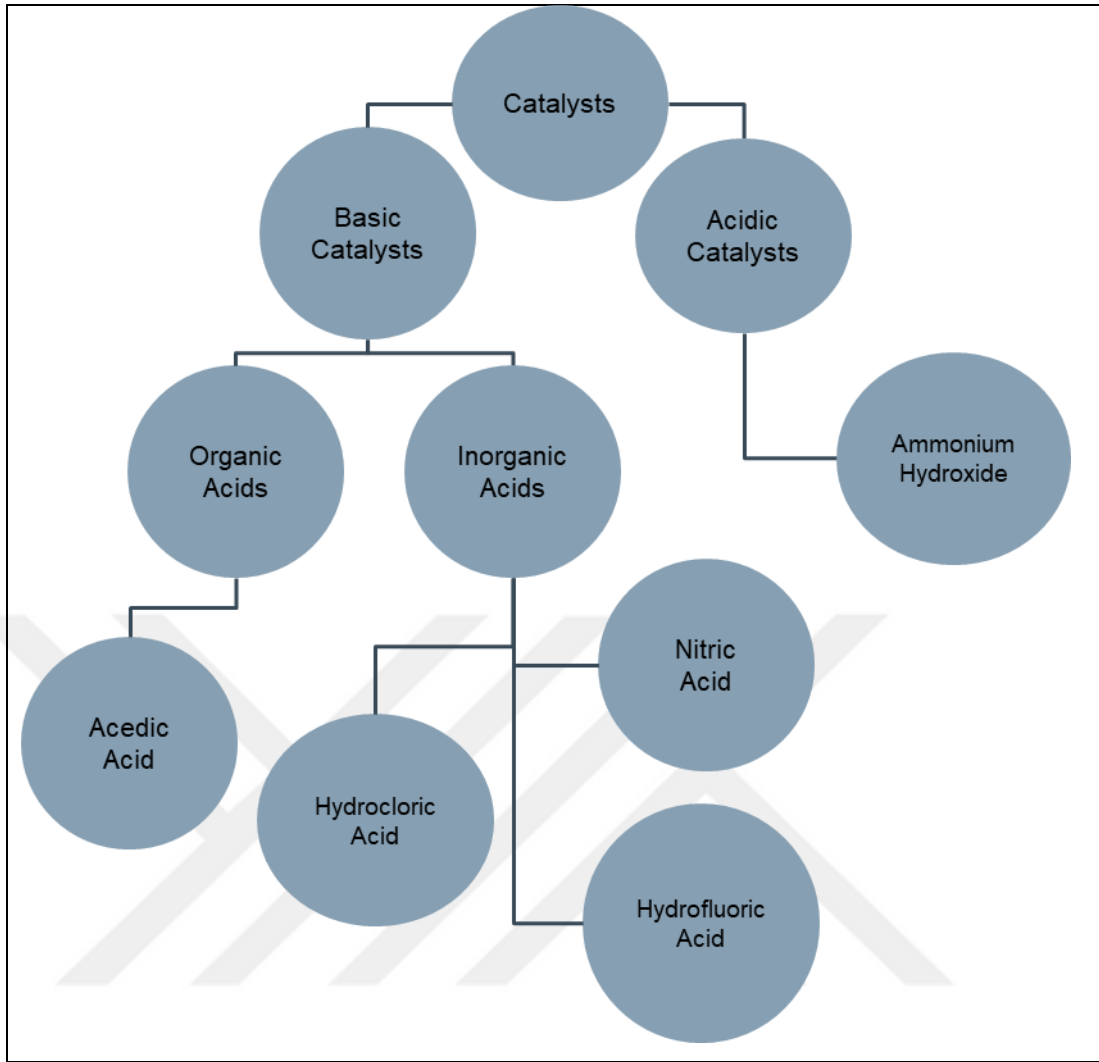


Figure 6.8: Some Types of Catalysts used for Sol-Gel method.

6.2.2. Hydroxyapatite

Hydroxyapatite (HAp) is a biocompatible and bioactive material which can be used as the repair of human hard-tissues. Hydroxyapatite is a calcium phosphate compound. It is part of the raw material called phosphoric rock. Hydroxyapatite is the main inorganic component of bones and tooth enamel.

Hydroxyapatite is mainly found in two forms, nanoHydroxyapatite powder and micron hydroxyapatite powder. The difference between the two powders is the size. The size of the hydroxyapatite nanoparticles is below 200 nm, while the micron Hydroxyapatite is in the range of 45- 90 microns. The surface area of Hydroxyapatite nanoparticles is about 9.4 m²/g, while Hydroxyapatite micron powder has a surface area of 120 m²/g [Ferraz et al., 2004], [Hing et al., 1999],[Lacefield, 1988]. The

greatest potential for bone substitution is shown by materials based on hydroxyapatite (HAp), $\text{Ca}_{10}(\text{PO}_4)_6(\text{OH})_2$, which is inorganic part of a human bone and can develop tight bonding with bone tissue, exhibits osteoconductive behavior, is stable toward bioresorption, and has no adverse effects on the human organism [Brown and Constantz, 1994]. The biological behavior of HAp ceramics depends on many factors, in particular, on their chemical and phase composition, microstructure, pore size, and pore volume.

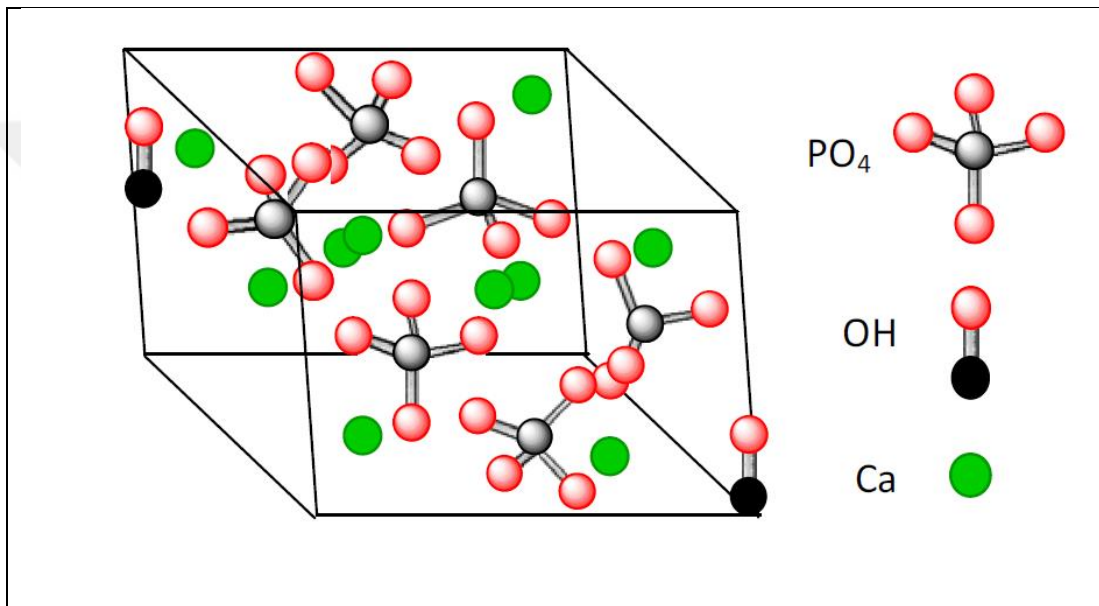


Figure 6.9: The structure of hydroxyapatite crystals.

Hydroxyapatite is the main mineral constituent to human bones and teeth structure, the major departures in composition being a variable Ca/P mol ratio is 1.67. HAp is hexagonal with space group P63/m, with lattice parameters $a = b = 9.4214 \text{ \AA}$, $c = 6.8814 \text{ \AA}$, $\alpha = \beta = 90^\circ$, $\gamma = 120^\circ$. (Elliott et al., 1973) The hexagonal structure is characterized by a six- HAp is not only a biocompatible, non-toxic, nonimmunogenic agent, non-inflammatory, additionally it is also bioactive [Ferraz et al., 2004], [Rujitanapanich et al., 2014]. HAp powders can be prepared by multiple techniques, various synthesis techniques have been Ca developed. These include hydrolysis of other calcium phosphates, hydrothermally, precipitation from aqueous solutions, sol-gel procedure and mechanochemical synthesis [Mobasherpour et al., 2007], [Shih et al., 2004], [Sopyan et al., 2008], [Zhang, 2007].

Sol-gel synthesis of HA ceramics has recently attracted much attention [Borello et al., 1992], [Itokazu et al., 1998], [LeGeros, 1988], [Liu et al., 2001]. The sol-gel method offers a molecular-level mixing of the calcium and phosphorus precursors, which is capable of improving chemical homogeneity of the resulting HA to a significant extent, in comparison with conventional methods such as solid state reactions [Young & Holcomb, 1982], wet precipitation [Osaka et al., 1991], [Salosarczyk et al., 2005], and hydrothermal synthesis [Yoshimura et al., 1994]. The versatility of the sol-gel method opens a great opportunity to form thin film coatings in a rather simple process, an alternative to thermal spraying which is currently widely used for bio- medical applications [Chai and Ben-Nissan, 1999], [Kloskowski et al., 2010], [Livage et al., 1998], [Montenero et al., 2000], [Stankevičiute et al., 2013].

6.2.3. Chitosan

Chitosan is a polysaccharide formed from the deacetylation of chitin, which is abundant in nature and obtained from the shells of insects. It has high biocompatibility and antibacterial properties. Therefore, chitosan is a suitable functional material for biomedical applications. Polysaccharides are high molecular weight condensation polymers. Polysaccharides are biomolecules naturally occurring at many different functions in living organisms. It has been shown to have many excellent properties for use in regeneration. Among the natural polymers, chitosan is widely used for applications in dentistry. It still being investigated for new usage areas [K. C. Gupta and Ravi Kumar, 2000].

Chitin is derived from the Greek word kiton, meaning armor discovered first in 1811. It was discovered in fungi in 1830 and later isolated from insects in the 1830s. In 1859, C. Rouget discovered chitosan. Chitin is a high molecular weight linear polymer of N-acetyl-D-glucosamine (N-acetyl-2-amino-2-deoxy-D-glucopyranose) units linked by β -D (1 \rightarrow 4) bonds. It is a highly insoluble material resembling cellulose in its solubility and low chemical reactivity. It is most abundant in crustaceans, insects, and fungi [K. C. Gupta and Ravi Kumar, 2000], [Mourya and Inamdar, 2008], [Nishimura et al., 1991].

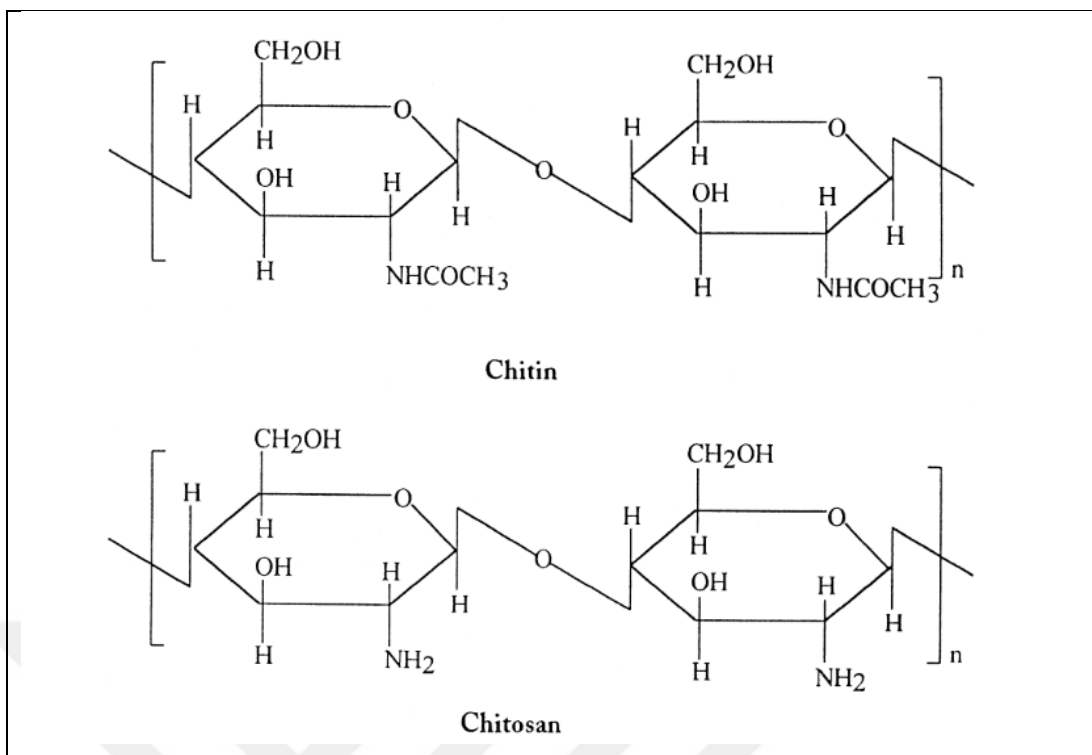


Figure 6.10: Crystal Structure of Chitin and Chitosan.

Chitosan is the N-deacetylated derivative of chitin, although this N-deacetylation is almost never complete. A sharp nomenclature border has not been defined between chitin and chitosan based on the degree of N-deacetylation [R. Gupta and Chaudhury, 2007]. Currently there are some attention has been paid currently to chitosan, because of its bioactivity, antibacterial properties and as a potential polysaccharide resource [Nishimura et al., 1991]. Although several efforts have been reported to prepare functional derivatives of chitosan by chemical modifications [Dutta et al., 2002], [Hirano et al., 1976], [Moore and Roberts, 1981], only a few examples attained solubility in general organic solvents. Chitosan is soluble in aqueous solutions of some acids; some selective N-alkylidenations [Hirano et al., 1976] and N-acylations [Dutta et al., 2002], [Hirano et al., 1976] have also been attempted.

7. SIMULATED BODY FLUID (SBF)

A simulated body fluid (SBF) is a solution with an ion concentration close to that of human blood plasma, kept under mild conditions of pH and identical physiological temperature [Kokubo & Takadama, 2006]. SBF was first introduced by Kokubo et al. in order to evaluate the changes on a surface of a bioactive glass ceramic [Uchida et al., 2003]. Later, cell culture media (such as DMEM, MEM, α -MEM, etc.), in combination with some methodologies adopted cell culture, were proposed as an alternative to conventional SBF in assessing the bioactivity of materials [Kokubo and Yamaguchi, 2019].

Table 7.1: Ion Concentrations of SBF and Human Blood Plasma.

ION CONCENTRATION(Mm)		
Ion	Blood Plasma	SBF
Na ⁺	142	142
K ⁺	5.0	5.0
Mg ²⁺	1.5	1.5
Ca ²⁺	2.5	2.5
Cl ⁻	103.0	147.8
HCO ₃ ⁻	27.0	4.2
HPO ₄ ²⁻	1.0	1.0
SO ₄ ²⁻	0.5	0.5
pH	7.2-7.4	7.40

Table 7.2: Regents for preparing SBF (pH:7.40, 1L).

Order	Reagent	Amount
1	NaCl	7.996 g
2	NaHCO ₃	0.350 g
3	KCl	0.224 g
4	K ₂ HPO ₄ ·3H ₂ O	0.228 g
5	MgCl ₂ ·6H ₂ O	0.305 g
6	1M-HCl	40 mL
(About 90 % of total amount of HCl to be added)		
7	CaCl ₂	0.278 g
8	Na ₂ SO ₄	0.071 g
9	(CH ₂ OH) ₃ CNH ₂	6.057 g

8. EXPERIMENTAL STUDIES

8.1. Materials and Methods

In this thesis, commercially pure powders of Si_3N_4 (Consist of 95% α , 5% β , and 1.4 wt. % O) (UBE, Japan), Al_2O_3 (Sky Spring, USA) and Y_2O_3 (Sky Spring, USA) were used as main powder compositions. Methyl ethyl ketone (MEK, Merck, USA) and its binary combination (%60: %40) with ethanol (EtOH) (purity 99.8%, Merck, USA) as azeotropic mixtures were used as solvents for tape-casting slurries. In addition, polyvinyl butyral (PVB, Chang Chun Petrochemical Co., Taiwan) as binder and sodium tripolyphosphate (STPP, Eczacibasi, Turkey) were used as dispersant, respectively. Polyethylene glycol 400 (PEG400, Merck, USA) and dibutyl phthalate (DBP, Plastifay Chem., Turkey) were tested as plasticizers. For final ingredient the Graphite V (Sky Spring, USA) used as pore maker.

For the synthesis of hydroxyapatite; calcium nitrate tetrahydrate ($\text{Ca}(\text{NO}_3)_2 \cdot 4\text{H}_2\text{O}$, $\geq 99\%$, Aldrich, USA) used as calcium precursor and triethyl phosphite ($\text{C}_6\text{H}_{15}\text{O}_3\text{P}$, %98 Aldrich, USA) as phosphorus precursor. The preparation of sols includes ethanol (EtOH) (purity 99.8%, Merck, USA) and distilled water. For the last process step, chitosan and acetic acid are used for the solution.

First step for the preparation of slurries, weighed amounts of Si_3N_4 , Al_2O_3 , Y_2O_3 , and STPP were ball milled for 8h in an azeotropic solvent (i.e., 60 vol% MEK/ 40 vol% EtOH) with Si_3N_4 balls. After the completion of the first milling process, a plasticizer and binder emulsion were added to the slurry and ball milled for 16h. For functionally graded structure single slurry is not enough. At this study 4 different type of slurries are prepared before the tape casting step. Each slurry has different ratios (%0, %8, %15, %20) of pore maker (Graphite V) which increases the pore ratio at each layer. After a homogeneous slurries was attained, the slurries were ready for casting.

Tape casting has performed at a MSE branded TC-0901AL model tape caster on a glass surface at a speed of 3 cm/s. The blade height was 250 μm . After drying at 25°C for 24 hours, tapes has been cutted into smaller pieces with 5 mm x 1 mm dimensions. The pieces from tapes with different pore maker compositions, were stacked on top each other. The pore content was systematically reduced from top to

bottom. Stacks with 40 layers (10 sheet with 4 composition) were prepared. These stacks were laminated at room temperature and cold isostatically pressed (2000 bar) to have optimum mechanical and metallurgical properties. After the pressing the green bodies are sintered for binder removal purposes at 1000°C for 1 hour. After binder removal process the substrate has been sintered at air atmosphere at 1500°C for 1 hour. To examine the adhesion of the coatings the substrates are etched with orthophosphoric acid (H₃PO₄, %85 Merck) at reverse flow system for 2 hours. With this final step, preparation of the substrates is completed.

Phosphorus precursor, triethyl phosphite sol was diluted in distilled water and some amount of absolute ethanol for hydrolysis. The mixture was sealed in a glass beaker immediately after solvent addition, then stirred vigorously. Due to the immiscibility between the phosphite and water, the mixture initially appears opaque, light being scattered by the emulsion phase. After approximately 30-40 minutes of mixing, the solution becomes clear. This change means the hydrolyzation of triethyl phosphite has been completed. A stoichiometric amount of 3M calcium nitrate tetrahydrate dissolved in distilled water. The amount of calcium nitrate precursor is calculated specifically and carefully to maintain Ca/P ratio of 1.67. After the complete mixture completed, the calcium nitrate solution subsequently added into the triethyl phosphite solution dropwise. The solution has been continuously stirred at room temperature about 24 hours before the coating process.

Dip-Coating process has been performed at laboratory type customized dip-coater. For the synthesis and coating of hydroxyapatite, dipping speed of 5 mm/min has been selected because of the sol to be embedded into the other layers. After the coating process completed the substrates are aged at room temperature for 24 hours. The hydroxyapatite coated functionally graded Si₃N₄ substrates sintered at 750°C for 1 hour.

For the final doping and coating, chitosan and acetic acid (CH₃COOH, ≥%99,8 Aldrich) solution has been prepared at room temperature, sealed with glass watch and stirred for 24 hours. After having the homogenous mixture, the coating performed at dip-coater with 5 mm / min speed. The coated substrates aged at room temperature for 24 hours and sintered at 250°C for 1 hour.

The HA and chitosan phase derived from the different precoating processes included substrates was detected using an X-ray diffraction (MAC Science, M18X)

with θ of 20-90. Scanning electron microscopy (SEM, Hitachi, Japan) was used for microstructural examination from the surfaces and the edges. Energy Dispersive Spectroscopy (EDS, MAC Science, M18X) analysis has been performed again from the surfaces and edges. Surface roughness analysis has been examined using profilometer (Veeco, DEKTAK 8 Adlanved Development Profiler) device for the substrates from 500x500 μ area, using 3 mg force and 32 profiles. Finally, the 3D surface roughness analysis are examined for coated substrates.

For bioactivity tests, Simulated Body Fluid has been prepared and substrates are dipped into the solution. Eventually, the substrates are pulled from SBF with; 0h, 24h, 72h, 144h time parameters and examined through SEM imaging and EDS analysis.

8.2. Preparation of Substrates via Tape Casting

For the first step of the tape casting process is; the preparation of the solutions. The main powder is Silicon Nitride and the solution is based on this powders properties. Relatively, %30 Silicon nitride is used for each prescription and other additions are added depending on the main powder. For silicon nitride to have smaller sintering temperatures yttrium oxide and aluminum oxide are added as sintering additives. Relatively, %2-3 yttrium oxide and %1-1,5 aluminum oxide is used for main powder composition for each prescription. Addition of dispersants is a major step for tape casting solutions. To have stable rheological properties of the solutions, dispersants are used commonly. The agglomerations that occur together with the water increase the viscosity of the suspension. Most importantly, it causes structural defects in raw strips. Therefore, dispersant selection to obtain low-viscosity suspensions with the quantities are very important. Sodium tripolyphosphate (STPP) is used for this purpose with %1,5 volumetric ratio. Methyl ethyl ketone (MEK) and Ethyl alcohol (EtOH) is used with the 6:4 ratio for solvent as every solution. To have the required mixture and viscosity, the solution is putted into the ball milling machine for 8 hours to have maximum homogeneity before adding other additives. Powders and additives are prepared for strip casting suspension with Glen Mills Inc. (Figure 8.2.1) brand ball mill to distribute the ingredients homogeneously. Silicon nitride balls are added to the solution to help solutions complete homogeneity.



Figure 8.1: Glenn Mills Inc. ball milling machine.

After the first part of the milling process, the other additives are added to the solution. In the suspension preparation process, polyvinyl butyral (PVB) is used as an alcohol-based binder. Dibutyl phthalate (DBP) and polyethylene glycol (PEG400) was used as plasticizers.

When the viscosity values of the suspensions depending on the shear rate are examined, it is seen that the lowest viscosity value was obtained in the suspension without additives. With the increase in the amount of solid load, the viscosity increased proportionally. 0% added of the lowest viscosity value in suspension, the highest viscosity value is in suspension with 30% additive has been measured for maximum and minimum shear rate.

The final solution is milled for 24 hours with the same milling machine. As mentioned above, the tape casting method is chosen for the production of functionally graded silicon nitride substrates. The tape Casting method has been completed using MSE TC-0901AL tape caster.

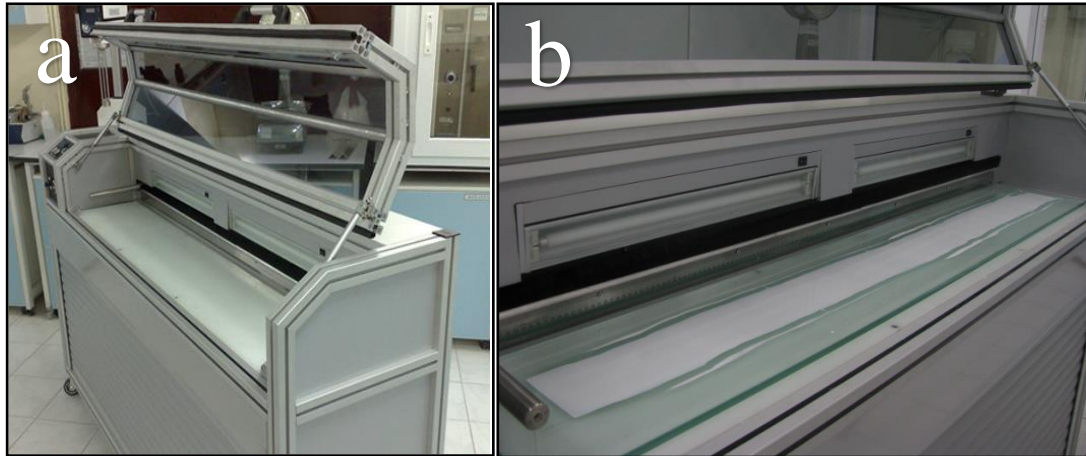


Figure 8.2: MSE TC-0901AL a)Tape Casting Device and b)Casting Example.

Tape Casting process has been completed at 3 mm/sec. The solutions that has been prepared 24 hours are charged into the doctor blade and the Casting has been completed for each solutions with different glasses.

Each solution has different amount of pore maker which is Graphite V. It can be clearly seen from the images that the amount of graphite makes the colour more darker. After the casting process, surface of the tapes are examined and checked for pin hole, shrinkage detect etc.

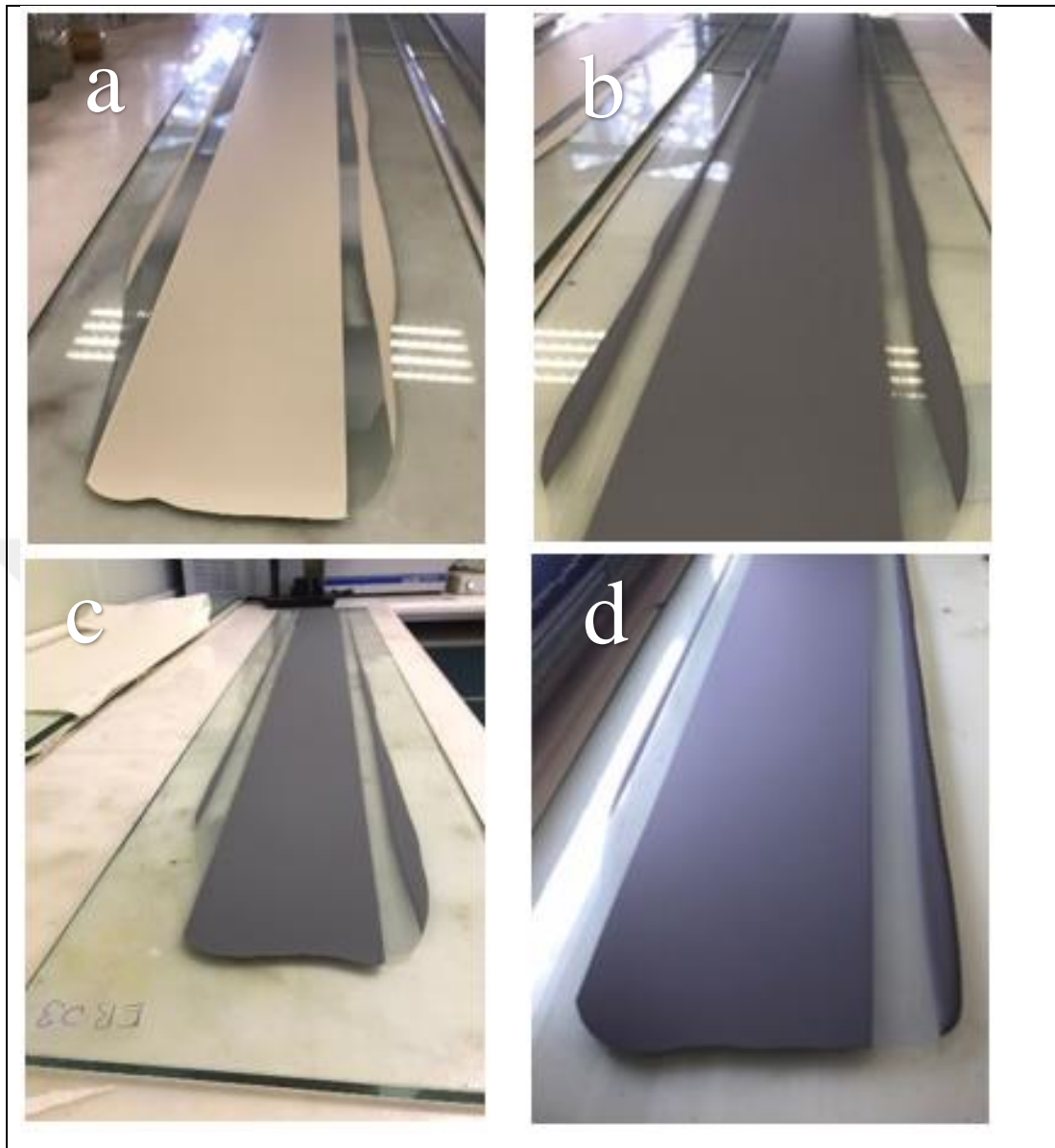


Figure 8.3: The tape casted film examples on glasses on increased Graphite V.
a) Bulk b) %3 Graphite V c) %5 Graphite V d) %8 Graphite V

After the casting process completed, the films are waited to dry at room temperature. The drying process shows us the final form of the tapes. The tapes are checked for any type of defects before the cutting and lamination step. The substrates are cutted from 1x5cm to have the desired surface area for the dip coating. The tapes are cutted with the required sizes and 10 tapes from each solution is cutted and laminated from the top to bottom depending on the pore maker ratio.

When the lamination is completed the substrate has 40 tapes with 4 different layers (Figure 8.4). After the cutting and lamination process, substrates are prepared to be vacuuming process and pressing.



Figure 8.4: a) The Lamination and b) Cutting process.

The pressing is one of the most essential process because it will determine the properties of functionally graded structure. Pressing also helps the lamination process by increasing binding between the tapes.



Figure 8.5: a) Preparation for Vacuuming b) After Cold Isostatic Pressing.

Pressing process has been completed at Quintus Tecknologies (Figure 8.6) branded CIP (Cold Isostatic Press) device. From the earlier works, it it proven that the

most ideal structure achieved at 2000 bar pressing. Which is why, only 2000 bar pressed structured are used for this study.



Figure 8.6: Quintus Technologies branded CIP device.

Heat treatment are the most essential and important part for the production of Functionally Graded Silicon Nitride using tape casting. For substrates usage at human body requires some binder removal process. Which is why the substrates are pre-heat treated at 1000°C to remove un-wanted chemicals. Binder removal process is very important not only because of the binders removal also the physical structure of the substrate. The process has been completed at 1000°C at 5°C/min heating rate for 1 hour at Protherm Heat Treatment Oven (Figure 8.7).



Figure 8.7: Protherm Heat Treatment Oven.

The sintering process is done after the binder removal process. Sintering of silicon nitride ceramics requires high temperature. Even with the sintering additives, the process needed to be completed at 1500°C for 1 hour. For heat treatment to be done homogenously the substrates are covered with aluminum oxide cups (Figure 8.8). The sintering needed to be completed at slow rate so the heating process is made at 1°C /min. Slow heat ratio is very essential for substrates to defend its firm structure. The bending and other deformations are very common at this type of materials.



Figure 8.8: Heat treatment process (Left) and final substrate (Right).

Once the sintering process is completed the the substrates becomes ready to coatings and other surface treatments. The substrates are prepared with the same method and parameters.

8.2.1. Surface Treatments

8.2.1.1. Grinding

The substrates surface normally doesn't require and treatments. In order to prevent bending, covering with silicon nitride powder required for the substrate. As it can be seen at figure below, the surface had to be lightly grinded to have smoother surface area.



Figure 8.9: Surface of the final substrates.

8.2.1.2. Etching

One of the chemicals used in etching silicon nitride is phosphoric acid. The etching process dependent on the concentration of orthophosphoric acid. Therefore, the reverse-flow etching system is used for this purpose. Samples thrown into orthophosphoric acid at room temperature and heated to the boiling point of 180°C. Etching has been done with, boiling orthophosphoric acid for 2 hours, then the substrates are adequately rinsed with distilled water at the appropriate temperature. Finally, washed and dried in an oven.



Figure 8.10: Reverse-Flow etching System.

Reverse-flow device is a setup allows water cooling of gas evaporation from a heated liquid system, which ensures that the concentration of the liquid is kept constant. Magnetic stirrer table with heat meter, crystallization vessel, glass balloon, condenser, pedestal holder, plastic hose and toy balloon are used.

The liquid to be heated is put into the glass balloon, combined with the condenser, and fixed to the holder. A liquid such as silicone oil, glycerin, paraffin is poured into the crystallization vessel and filled up to a certain level. The neck of the balloon is closed with a stopper. Temperature controlled thermometer of the tray is periodically inserted through one neck of the balloon for temperature control. The hose connected to the lower end of the condenser is connected to the tap, to the upper end of the condenser. Water inlet-outlet is provided by connecting the connected hose to the outside. By adding a toy balloon and a squeezing piece so that the plug does not come off in the possible gas outlet the volume is created to provide flexibility.

Etching has been done to ensure adhesion on the substrate surface. As can be seen in the experimental data, for the chitosan coating process, etching was quite efficient to provide the necessary adhesion.

8.3. Synthesis of Hydroxyapatite via Dip-Coating

8.3.1. Preparation of the Sols

In the preparation of the initiators for sols in all trials, as a calcium precursor calcium nitrate tetrahydrate ($\text{Ca}(\text{NO}_3)_2 \cdot 4\text{H}_2\text{O}$, $\geq 99\%$ Fluka), as phosphorus precursor triethyl phosphite ($\text{C}_6\text{H}_{15}\text{O}_3\text{P}$, 98% Aldrich) was used. As a solvent for triethyl phosphite distilled water was used and the hydrolysis time was fixed at 24 hours. Calcium precursor was dissolved in ethyl alcohol ($\text{C}_2\text{H}_5\text{OH}$, $\geq 99.8\%$ Aldrich).

In the sol-gel synthesis of hydroxyapatite, the pH of the initiator sol to be very low may slow down the condensation reactions and may affect phase purity.



Figure 8.11: Preparation of the Sols at room Temperature.

8.3.2. Aging of the Sols

All prepared sols were aged at room temperature for at least 24 hours. The prepared sols were checked regularly to prevent precipitation. Air inlet and outlet were not allowed by covering the top of the beaker. The mixture was aged for exactly 24 hours at a rotational speed of 300 rpm.

8.3.3. Coating Process

The samples were coated by dip coating method. The tensile speed in the dipping process is 5 mm/min for all trials. A handmade mechanism is used in the dipping coating process and all coatings have the same dipping distance, dipping speed and holding time. The dip coating assembly is shown in the figure below.



Figure 8.12: Dip-Coating Device and Process

8.3.4. Drying

Drying of the samples is a very important step for the adhesion of the coatings to the surface. For this reason, the coated samples were tested in a 24-hour period with Nüve FN 120 Dry Air or in the open air.

8.3.5. Calcination

Dried samples were calcined at 750°C for 1 hour. Dry gels obtained by evaporation of the solvents of the sols. After drying and calcination processes, the samples are shown in the image below.



Figure 8.13: Substrates after the coating and calcination.

8.4. Coating of Chitosan via Dip-Coating

The same steps of the previous coating process were used in the chitosan coating process. In this context, the differences are explained with visuals.



Figure 8.14: Preparation of Chitosan Sols at room temperature.



Figure 8.15: Coating before the sintering process with different parameters.

8.4.1. Sintering of Chitosan Coated Substrates

Chitosan is a polymeric material due to its structure. Therefore, it shows decomposition behavior at high temperatures. Since it is known that the decomposition temperature is between 270-300°C, the sintering process was carried out for 1 hour at 250°C with 1°C/min heat rate for all samples. After the sintering process, the samples were ready for the necessary tests.

8.5. Preparation of Simulated Body Fluid (SBF)

Making Simulated Body Fluid prepared by reference of Kokubo et al. In the preparation phase, all materials are new and first use. Taking into account all the necessary parameters, regular pH measurements were made and operations were carried out. The prepared setup is given in the figure below.

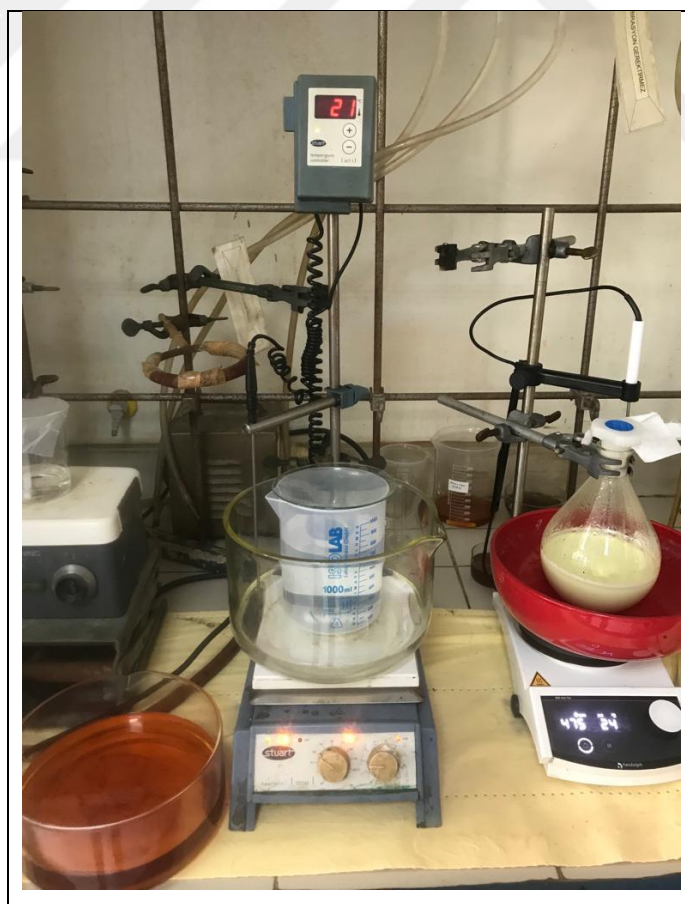


Figure 8.16: Preparation of Simulated Body Fluid.

After applying the required parameters, 1 liter of SBF liquid was kept in the refrigerator for 1 week and was used after observing that there was no precipitate.



Figure 8.17: Immersion of samples in SBF.

9. RESULTS AND DISCUSSIONS

9.1. Characterization of the substrates

The preparation of the slurries is the most essential part of tape casting process. For slurries to have the required viscosity and castability solution needs to be perfect. Otherwise, the casted materials can have many defects (pin-hole structure, gum-like structure, etc.). For functionally graded structure four different solutions has been prepared with different pore maker additions.

The XRD result (Fig. 9.1) shows that the main silicon nitride powder is a combination of α -Si₃N₄ and β -Si₃N₄ crystal structure but mostly α -Si₃N₄. BET analysis (Fig. 9.2) shows that the silicon nitride powder has one distinct size population (100-900 nanometers), which is optimal for tape casting process. The particle morphology was determined using SEM analysis (Fig. 9.3). For the main powder, SEM images shows inhomogeneous distribution with different degrees of aggregation between the primary particles. SEM images well correlates with particle size determined in powders by BET.

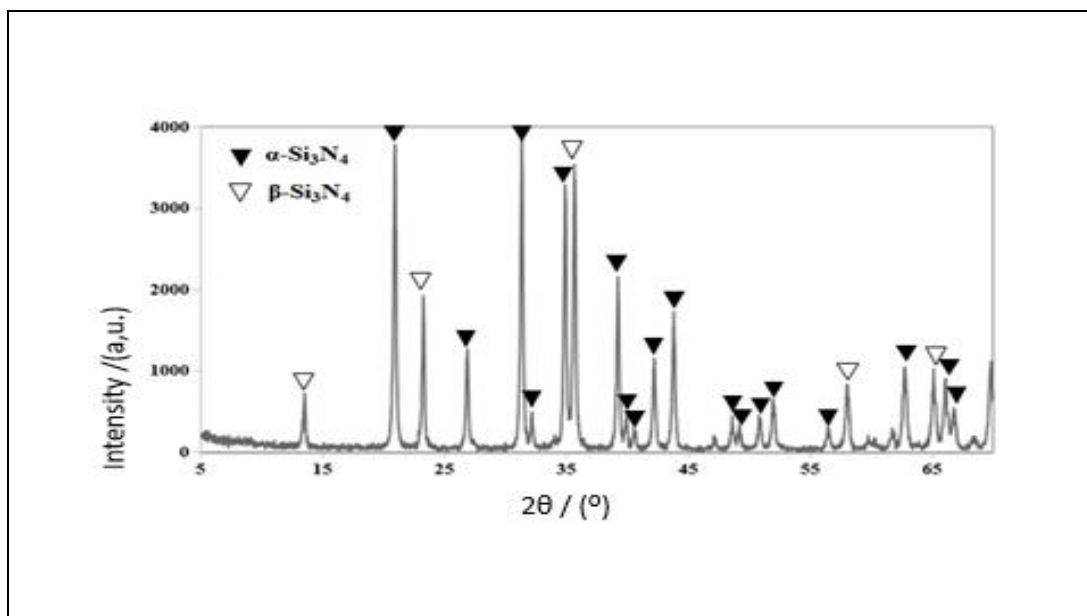


Figure 9.1: XRD analysis of UBE silicon nitride powders (Intensity vs. 2 θ degree).

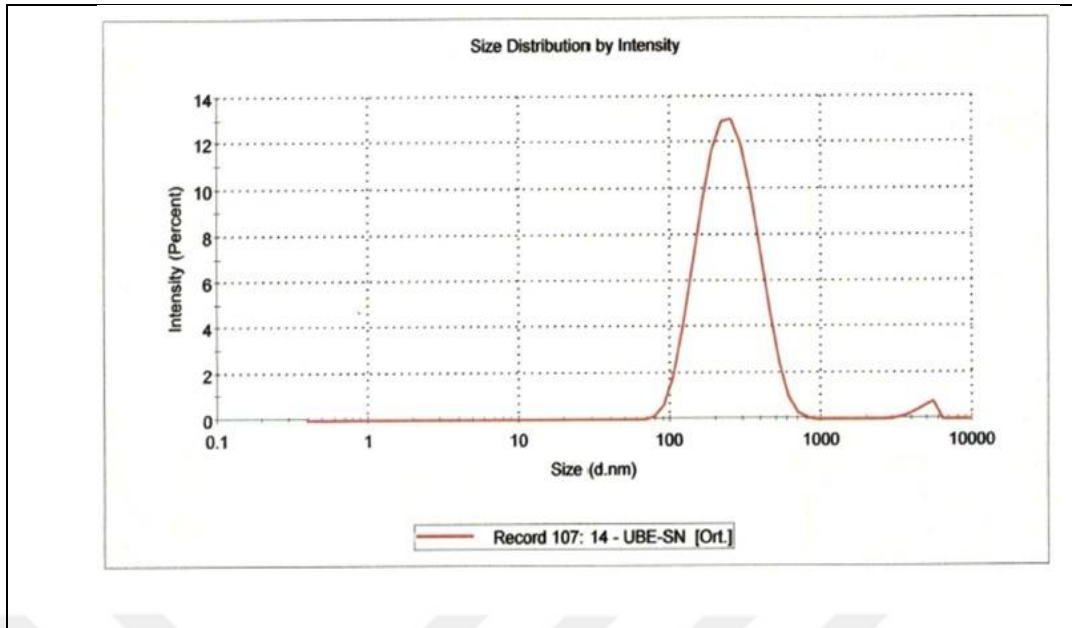


Figure 9.2: BET analysis of UBE Silicon Nitride powder (Intensity vs particle size distribution).

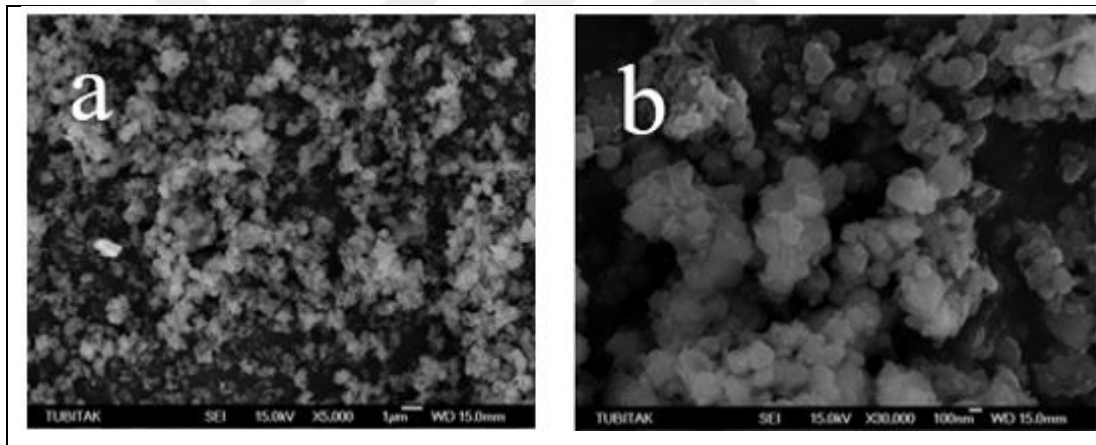


Figure 9.3: SEM Results of the Silicon Nitride powders. a) x5000 b) x30000

The XRD results indicates the mixed crystal structure of the powder is affected as inhomogeneous structure which can be seen from the SEM results. This inhomogeneity can affect the main structure, slurry properties, mechanical properties but as for this study it is desired because of the pore size and distribution. For the coating and doping part, the porous structure helps the coated materials to penetrate inside of the substrates. This eventually helps enhancing the bioactivity of the material and its ability to be doped and coated with other additives for other desired properties.

The SEM images of the substrates after the sintering process from the section can be seen from the Figure 9.4. (a and b images). It can be seen that the materials has

functionally graded structure. In addition, it is observed that the porous structure of the samples is more in the upper layers. This porous structure is very efficient for the formation of the coating. In addition, the porosity of the structure will allow additional chemicals to penetrate from the surface and dope, apart from the coating.

From Figure 9.4. (c and d images), it is observed that after the etching process is performed, the surface of the material has reached the desired roughness, although the amount of pores on the surface has decreased slightly. SEM image taken from the surface (image d) showed the heterogeneity in the surface structure.

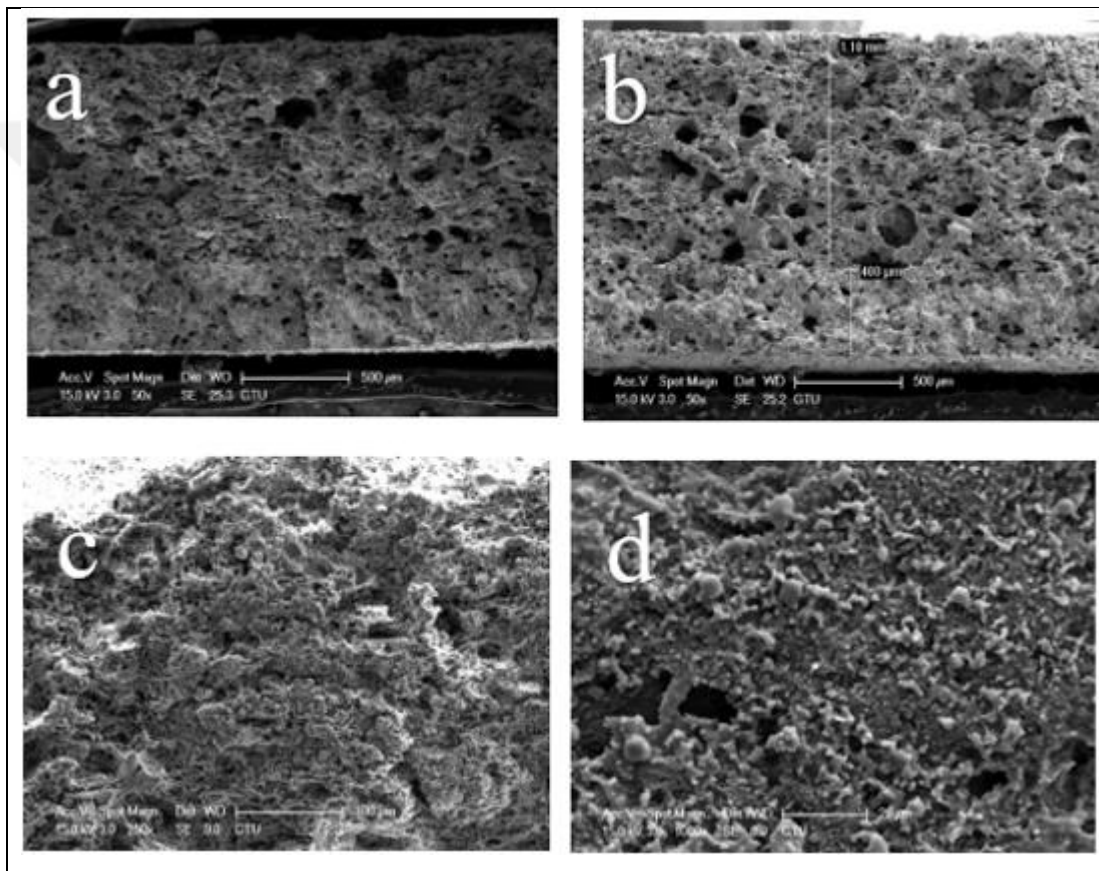


Figure 9.4: SEM images of the substrates. a) and b) shows the section without etching. c) shows etched substrate from section. d) shows the surface of the etched substrate.

9.2. Characterization of Synthesis and Coatings of Hydroxyapatite

In the process of dip coating of hydroxyapatite coatings, the preparation of a correct sol is the most important part. The coating process is basically based on simple mechanics. When a correct sol is prepared, the results to be obtained are only evident with some specific test methods. For this reason, SEM, XRD and Profilometer tests were performed on the substrate materials.

SEM images of the etched and unetched samples are shown below. In Figure 9.5, a and b, it is observed that the porous structure of the unetched sample is preserved, but the pores are almost completely filled. It has been noted that closing the pores of this structure may cause problems in the next coating and reduce adhesion. In figures c and d, SEM images of the etched substrate material coated with hydroxyapatite are given. It has been observed that there are few pores in the structure. It has been noted that these voids can create a suitable environment for the next coating. In addition, at figure 9.5: image c, a 3-dimensional hydroxyapatite network can be clearly observed in the SEM images of the structure. In the light of this information, there was a need to obtain XRD results from the samples in order to obtain a clear result.

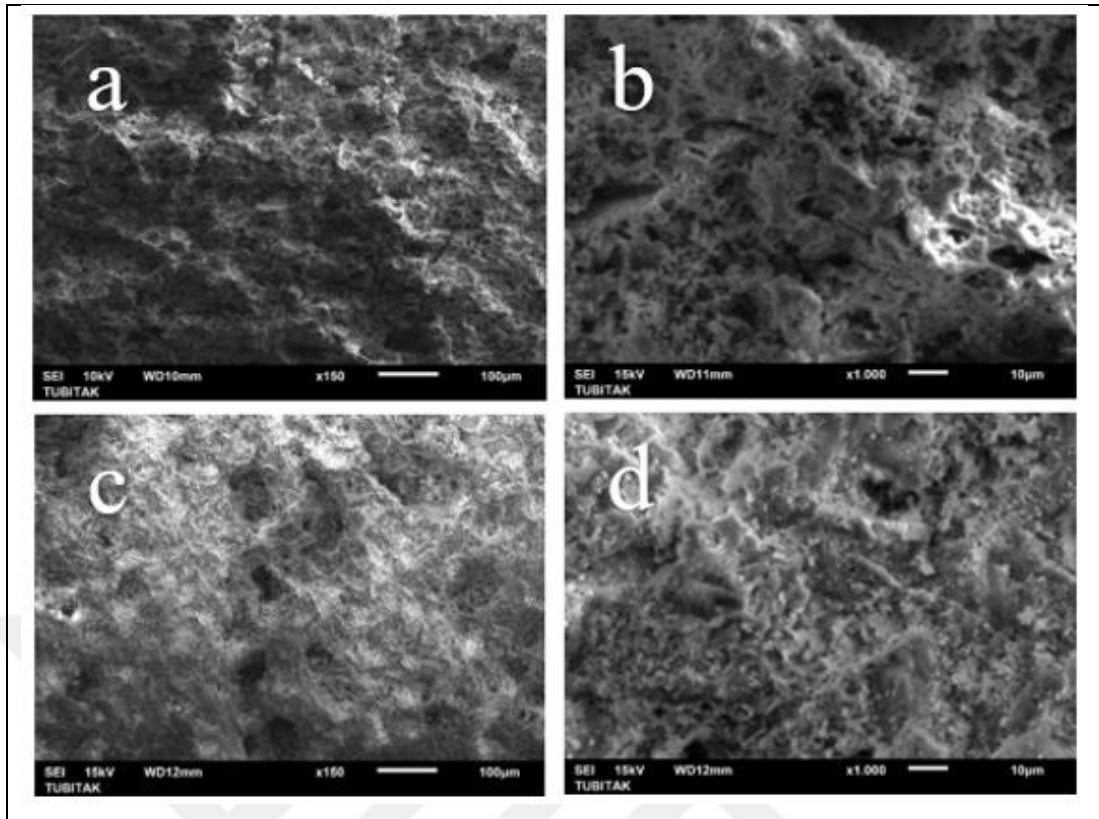


Figure 9.5: SEM images of HAp coated substrates from section. a) and b) shows unetched sections. c) and d) shows etched surface.

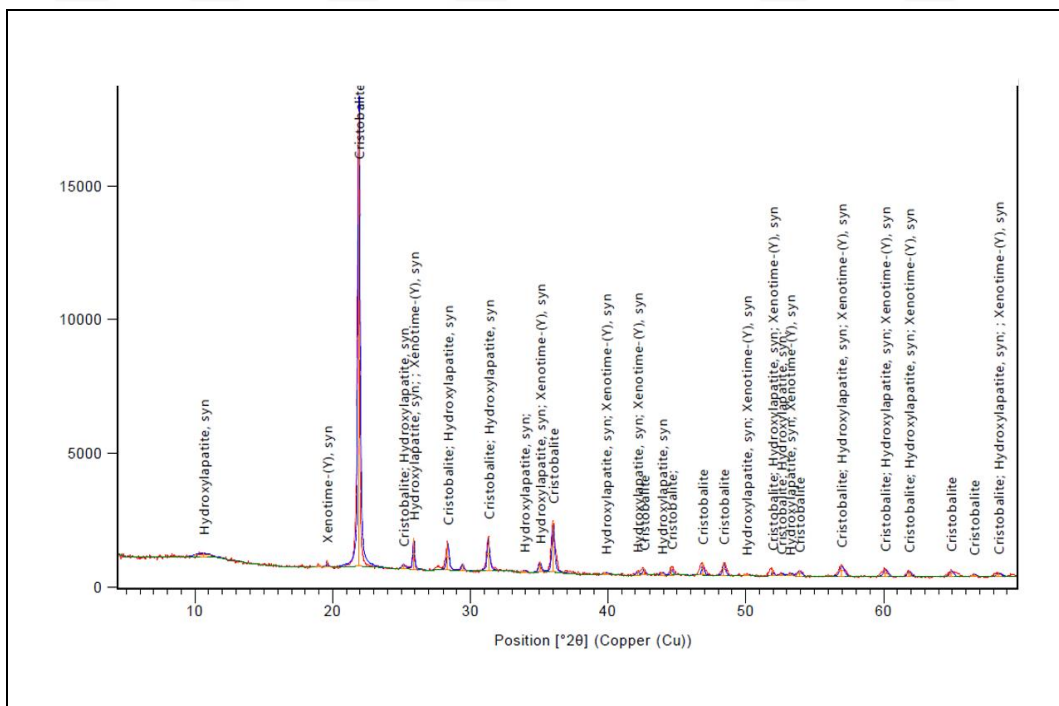


Figure 9.6: XRD Results of unetched HAp coated substrate.

XRD results were taken separately for etched and unetched samples. When the results were examined, it was observed that XRD results gave the required hydroxyapatite peaks at 10-11, 26-27, 34-35, 38, 45, 50 2θ angle (Figure 9.2.2 and 9.2.3). Although there is a slight difference in peak intensities, it has not been calculated separately. In the light of these results, it was decided that the etching process did not have a noticeable effect on the first coating. However, the peaks showed stronger intensities in the etched sample.

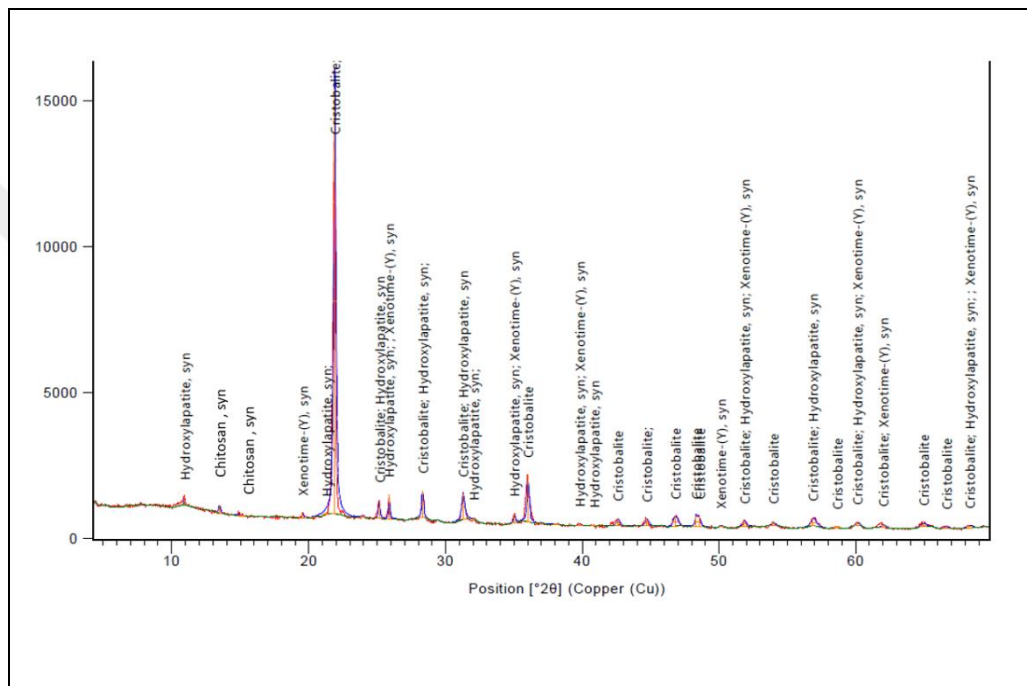


Figure 9.7: XRD Results of etched HAp coated substrate.

It was expected that the coated surfaces would give deeper roughness values in the surface roughness values measured in the profilometer. The results obtained were interpreted on the pre- and post-coating measurements of etched and unetched samples. 3D maps were extracted. The results gave the expected values and the roughness values of the desired coatings on the surfaces were observed.

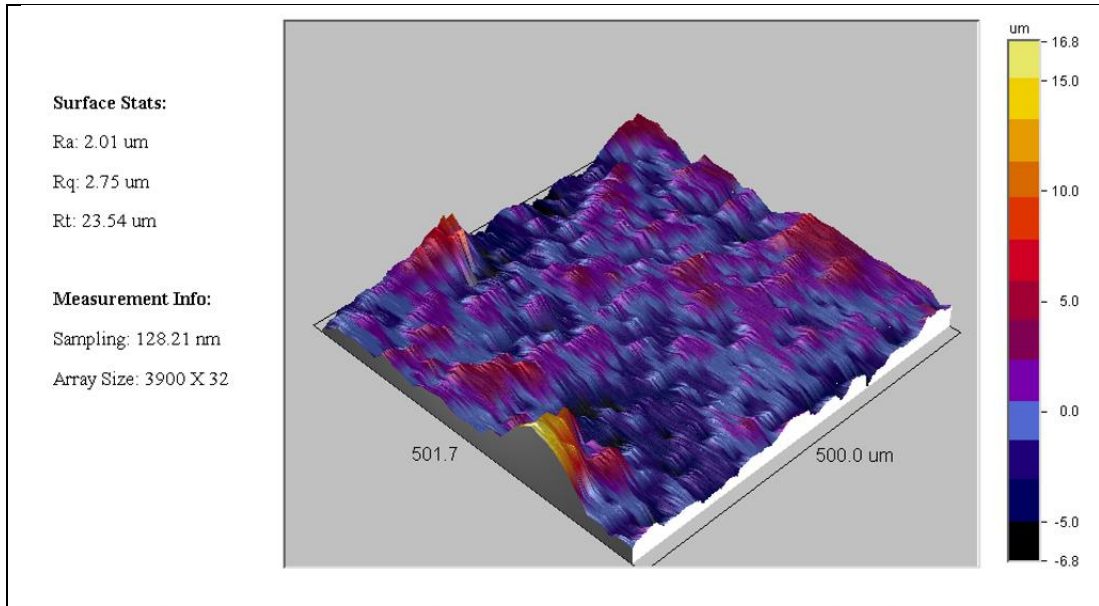


Figure 9.8: 3D Mapping of Surface Roughness for unetched and uncoated substrate.

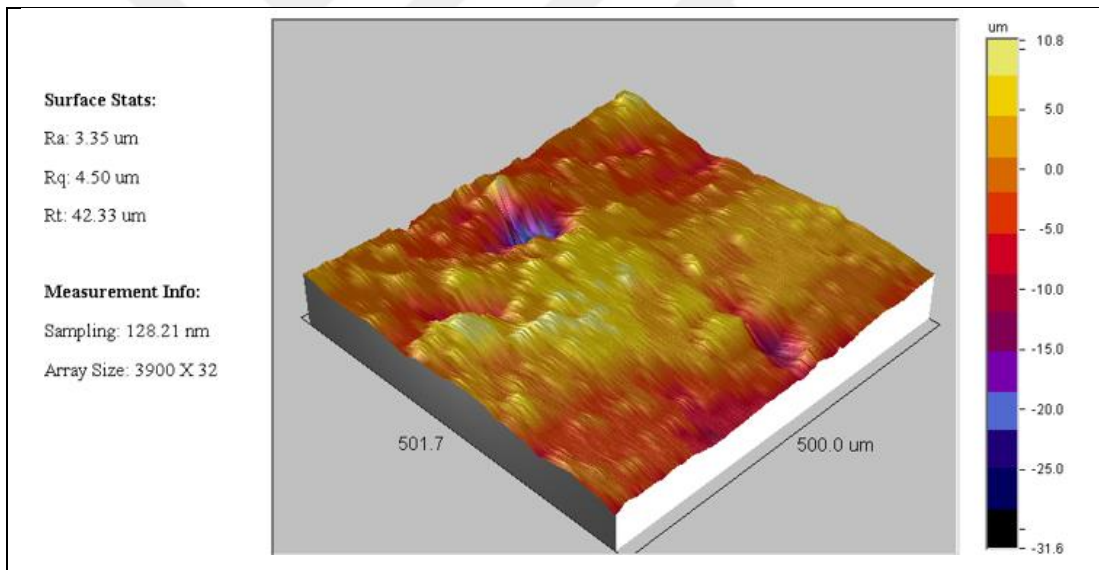


Figure 9.9: 3D Mapping of Surface Roughness for unetched and coated substrate.

As seen in the images above, there is a clear difference between Ra and Rt values. The difference between Ra and Rt values indicates that the coated surface has higher depth values. According to these results, it has been clarified that the hydroxyapatite synthesis and coating has been achieved successfully in unetched samples.

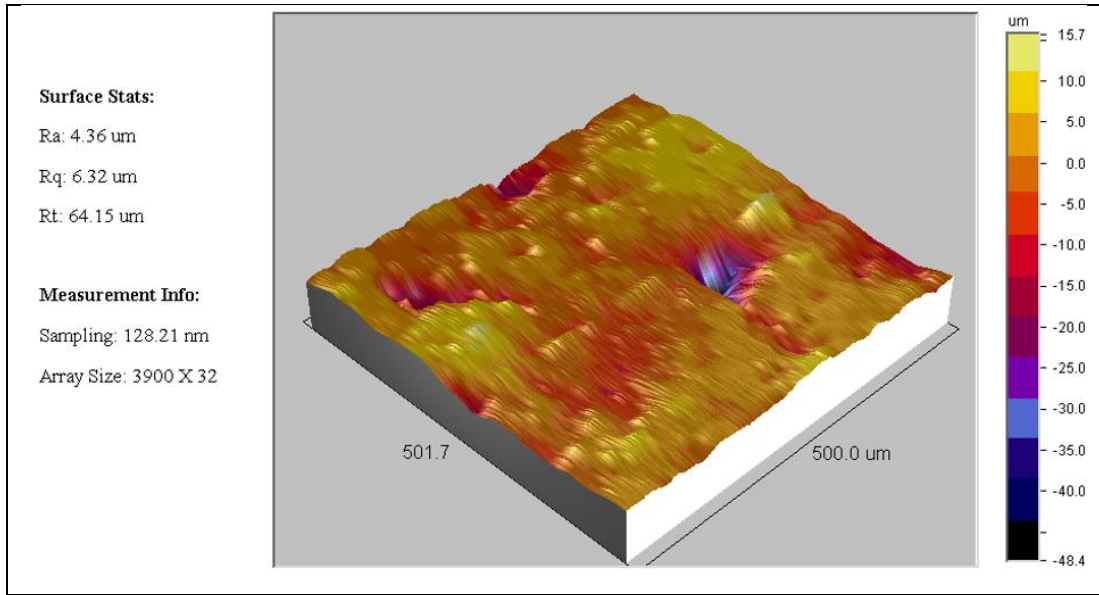


Figure 9.10: 3D Mapping of Surface Roughness for etched and uncoated substrate.

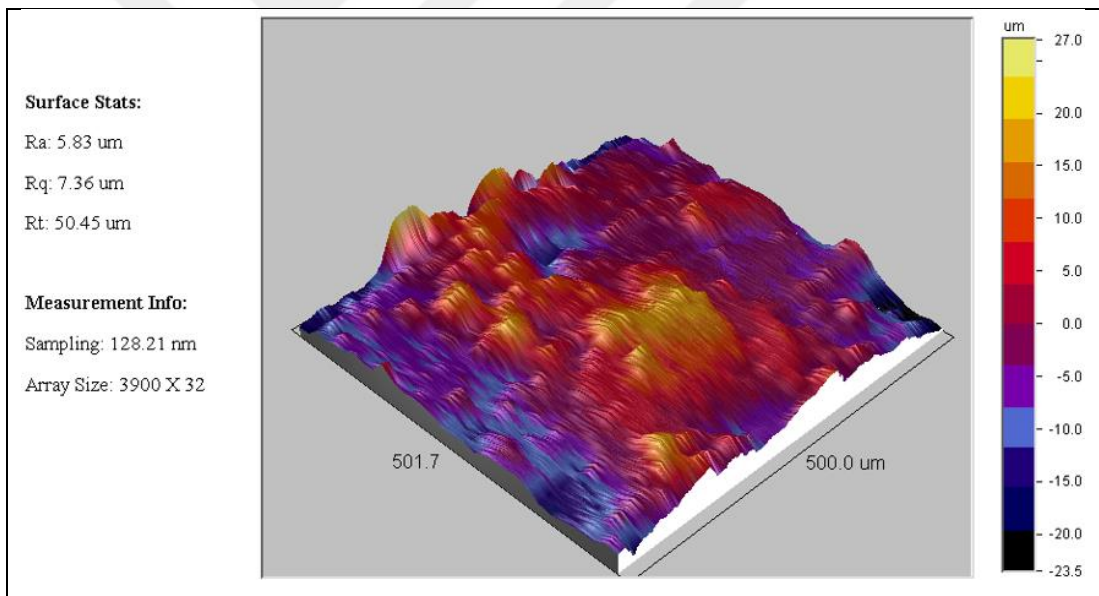


Figure 9.11: 3D Mapping of Surface Roughness for etched and coated substrate.

As seen in the images above, there is a clear difference between Ra and Rt values. This difference is also noticeable in the samples with and without etching. The difference gives us an idea about the surface roughness required for the next step. The difference between Ra and Rt values shows that the coated surface has higher depth values. According to these results, it has been clarified that the hydroxyapatite synthesis and coating was successfully achieved in etched samples.

9.3. Characterization of Coatings with Chitosan

Chitosan coatings are frequently encountered in the literature due to their compatibility with hydroxyapatite. However, functionally graded materials are as difficult to coat as they are to produce. For this reason, in this thesis, functionally graded and hydroxyapatite coated samples were coated with chitosan to increase bioactivity. After the sol containing chitosan and acetic acid was prepared and aged for 24 hours, the coating process was started.

The samples were coated by keeping the coating parameters constant with the dipping method used in the previous coating applications. The samples, which were coated by dipping, were dried for 24 hours and oven processes were started, and then they were subjected to SEM, XRD and Profilometer tests.

A very dense structure was observed in the SEM images taken after the coating processes.

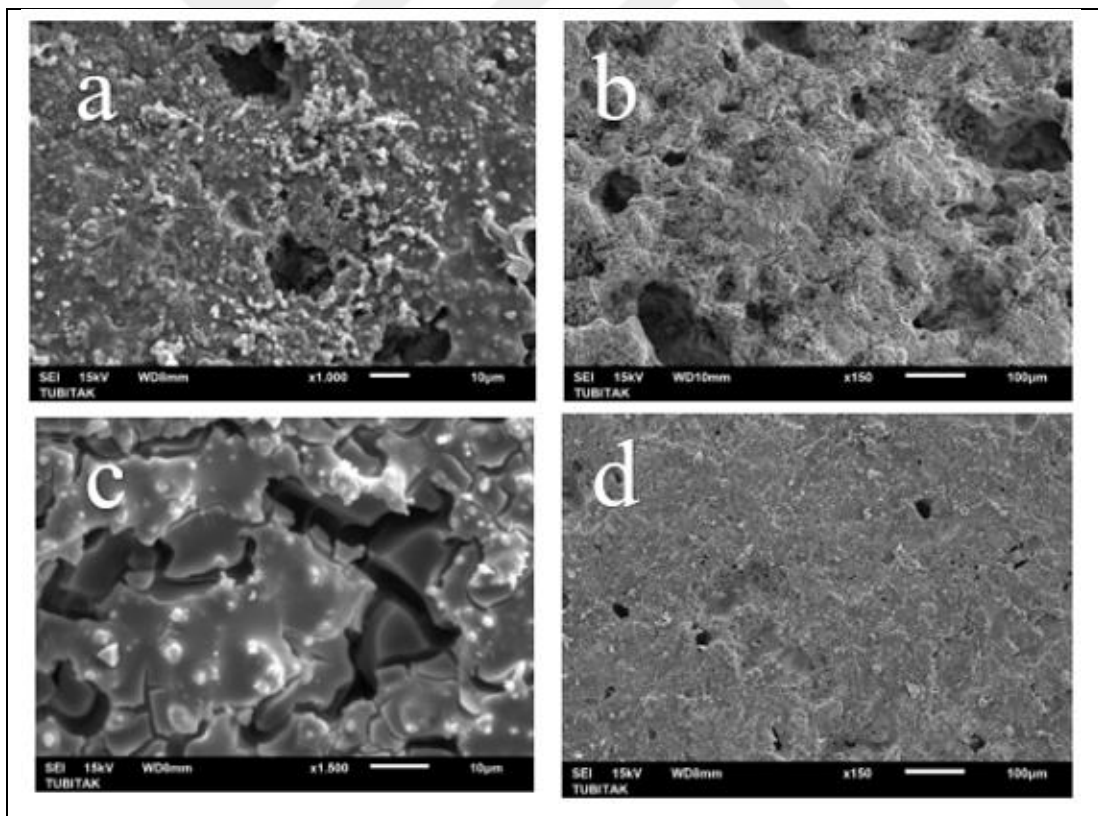


Figure 9.12: SEM images of HAp-Chitosan coated substrates a) and b) is unetched. c) and d) is etched.

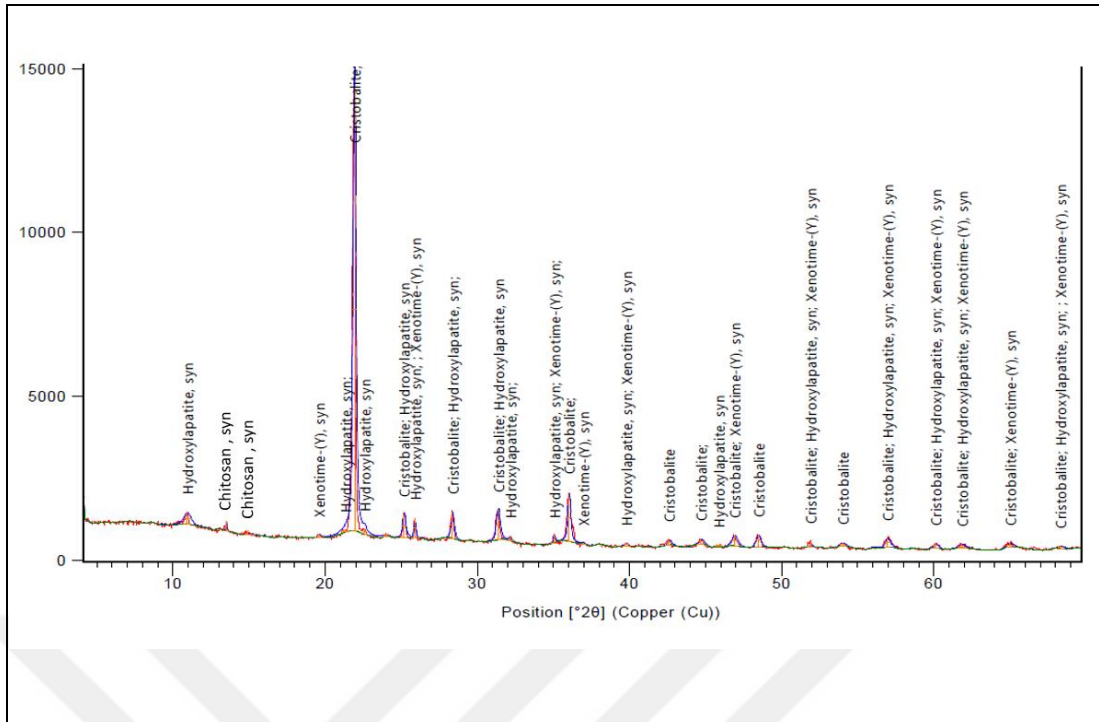


Figure 9.14: XRD Results of etched substrate after chitosan dipping.

Based on these results, the effect of cautery on chitosan adhesion was observed as predicted. The effect of etching on the adhesion created chitosan peaks on the surface, albeit a small amount. The surface roughness maps taken to measure the surface properties of the coatings are below.

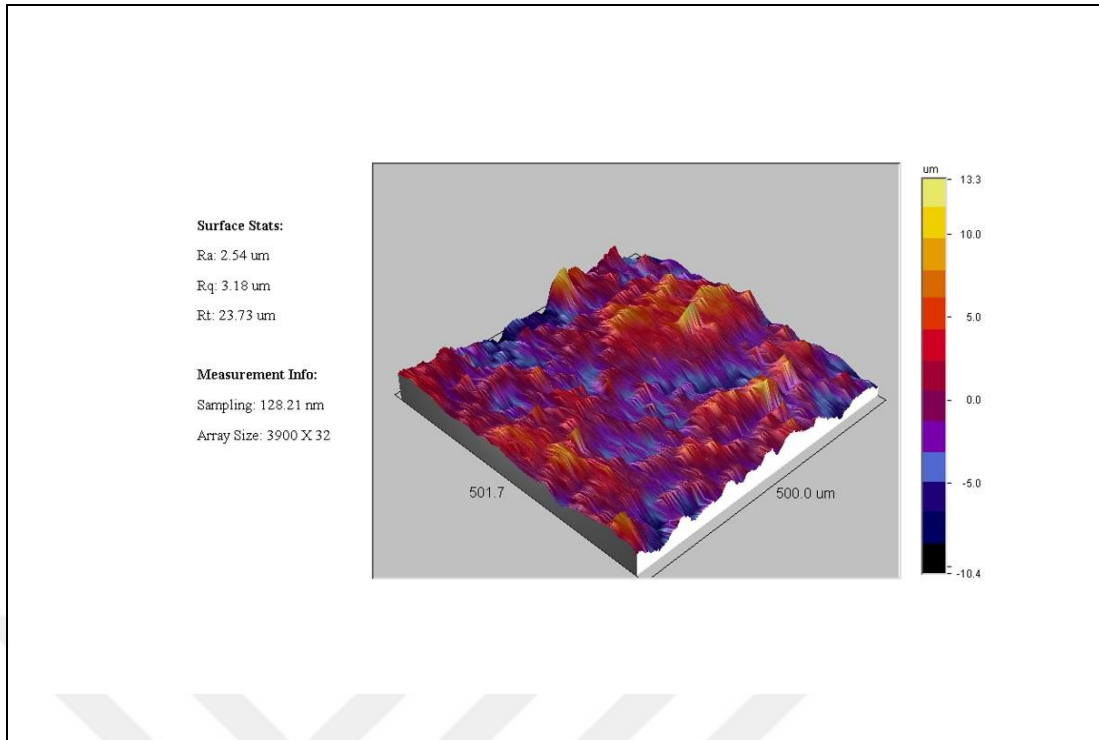


Figure 9.15: 3D Mapping of Surface Roughness for unetched and chitosan coated substrate.

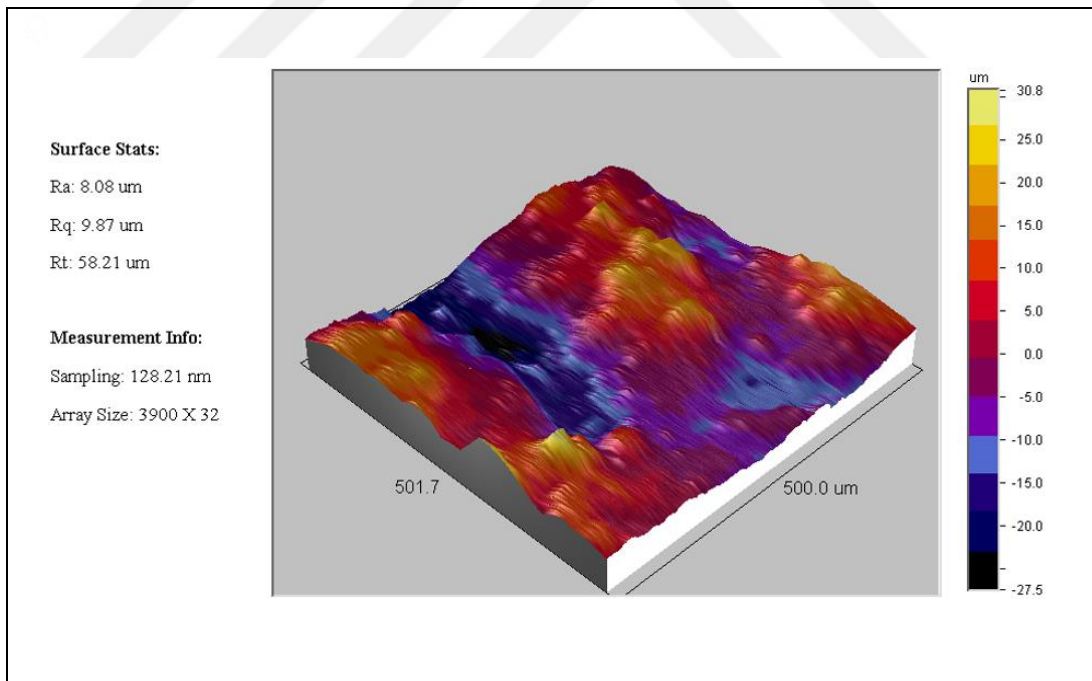


Figure 9.16: 3D Mapping of Surface Roughness for unetched and chitosan coated substrate.

As observed, from the surface roughness results obtained, it was observed that the roughness values in the figure 9.3.5, where the chitosan coating took place, were quite large compared to the roughness values of the unetched sample. Based on this information, the bioactivity test was started.

9.4. Bioactivity Tests using Simulated Body Fluid

In order to determine the bioactivity of the coated substrates, it was preferred to keep them in simulated body fluid for certain periods. In this context, SEM images of the samples were taken at 24h, 72h and 144h time intervals and analyzes were made. Apatite layer was expected to form on the surfaces in the images taken and the images were interpreted in the light of this information. SEM images are shown in figures below.

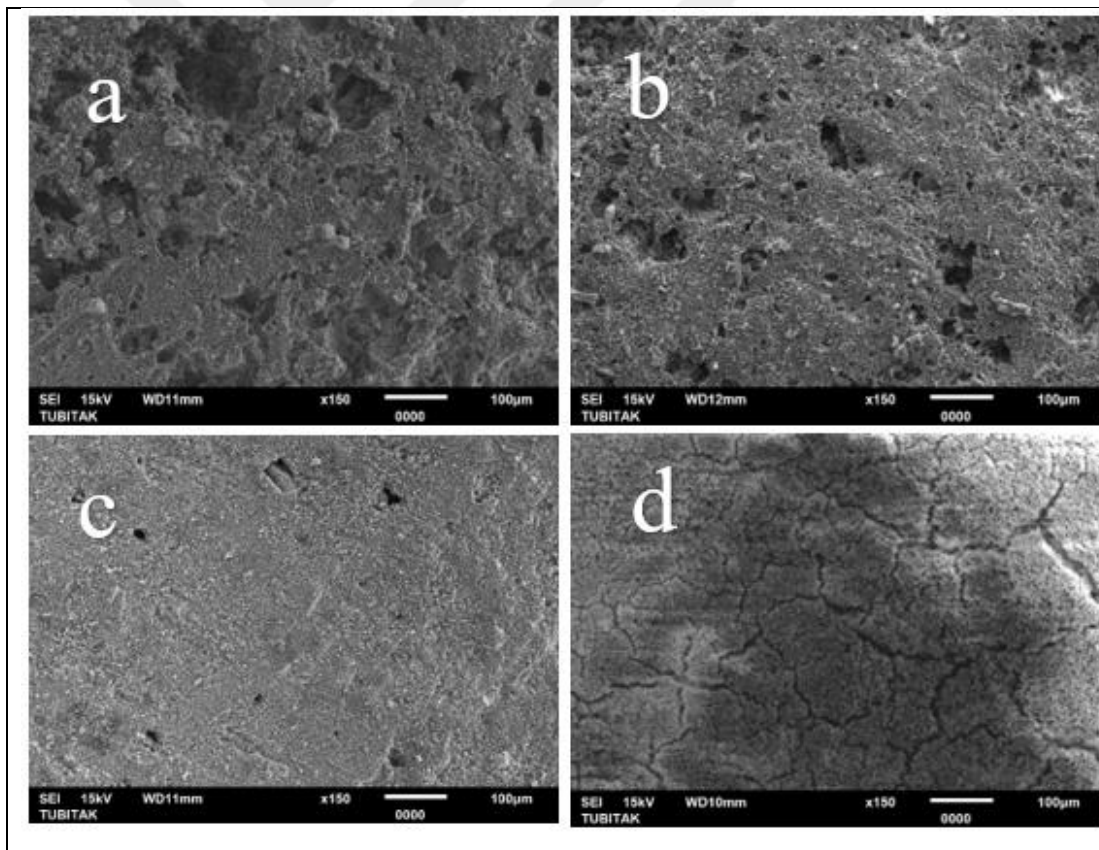


Figure 9.17: SEM images of substrates at SBF for 24 hours. a) Without coating. b) Unetched HAP coated. c) Etched HAP coated d) HAP-Chitosan coated

Uncoated sample, hydroxyapatite coated unetched and etched sample, chitosan and hydroxyapatite coated samples are observed in the above images. As observed from the image a, it was observed that no layer was formed on the uncoated sample and the lower hydroxyapatite peak in the unetched samples, as observed from the XRD results, resulted in less apatite layer in the image b. An apatite formation was clearly observed in the etched hydroxyapatite coating. It is seen in figure c, that almost the entire structure is covered in the images. Finally, in image D, a thick apatite coating is observed on the surface. Only within these visuals, it was concluded that the chitosan coating greatly increased the formation of apatite on the surface.

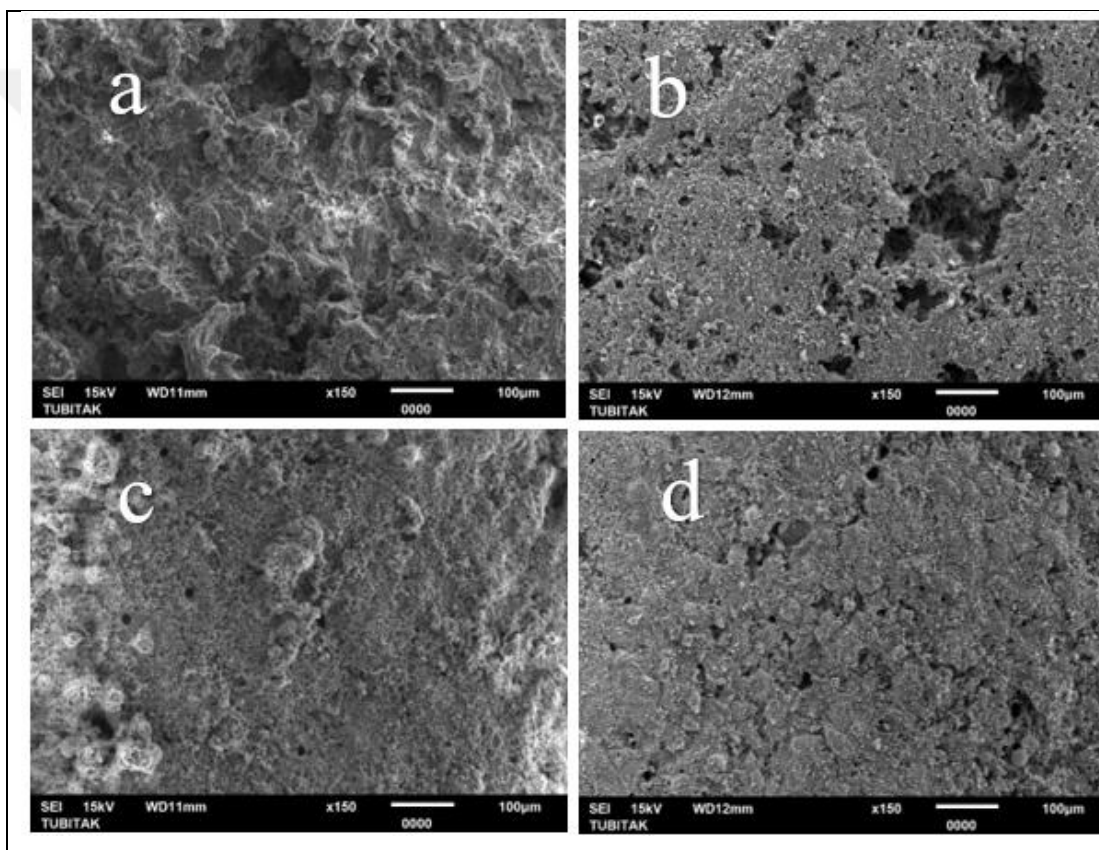


Figure 9.18: SEM images of substrates at SBF for 72 hours. a) Without coating. b) Unetched HAp coated. c) Etched HAp coated d) HAp-Chitosan coated

In the images after 72 hours, 3D structure was observed. Except for the first sample, the apatite structure is seen in more detail in the other samples. A denser deposited structure was observed in the samples with chitosan coating compared to the samples that were kept for 24h. As a physical observation, it was observed that the chitosan coated structure turned the transparent structure to white in SBF.

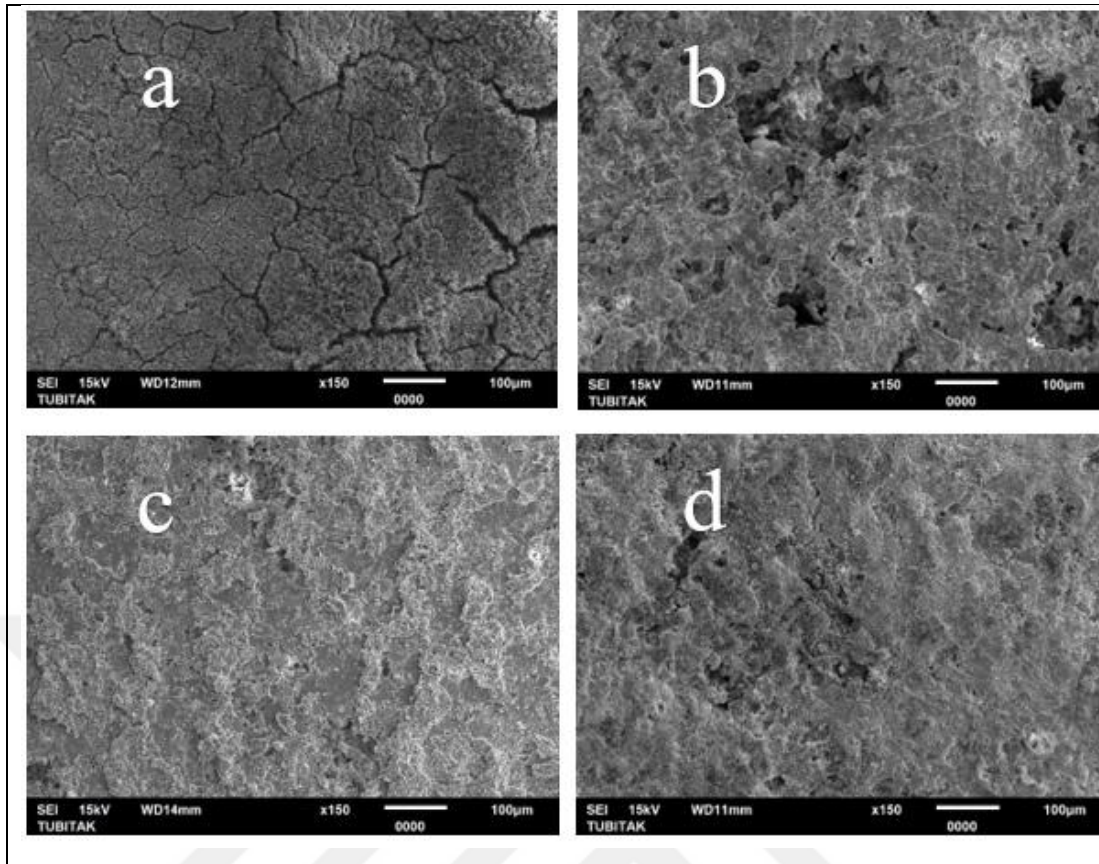


Figure 9.19: SEM images of substrates at SBF for 144 hours. a) Without coating. b) Unetched HAp coated. c) Etched HAp coated d) HAp-Chitosan coated

On the other hand, it was noted that in the samples that were kept for 144 hours, there was a physical accumulation in the uncoated sample, but it was poured on any contact. Apatite formation is observed in unetched samples, but the surface is not completely covered. Porous gaps are still observed. In the etched sample, the surface is completely covered. A very thick 3-dimensional layer is observed on the chitosan-coated sample surface. Only in line with these observations it was concluded that the bioactivity was greatly increased.

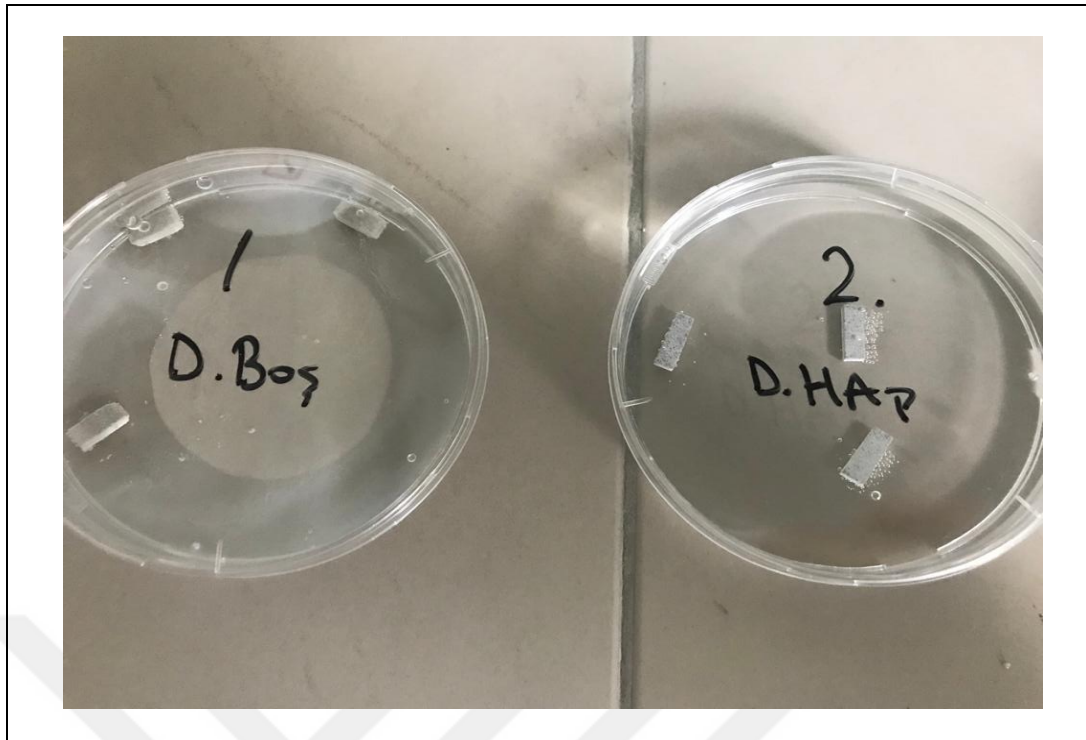


Figure 9.20: SBF tests of substrates of uncoated and etched coated substrates. Uncoated (left), Unetched HAp coated(right).

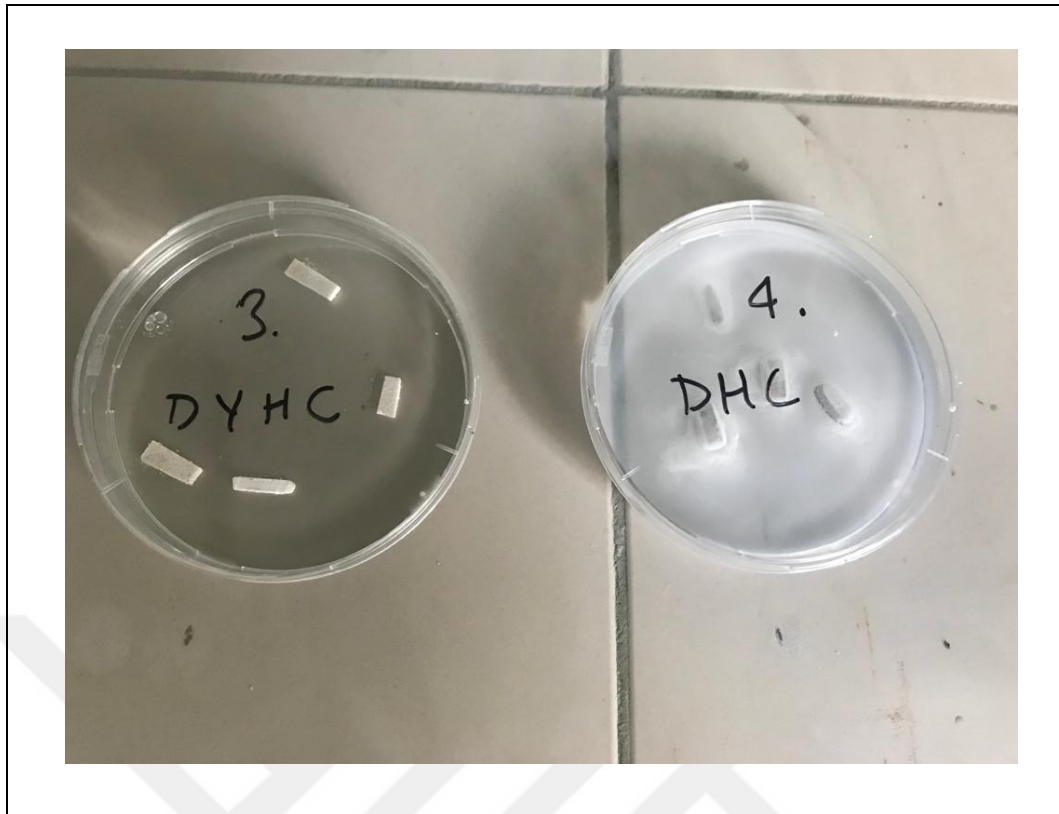


Figure 9.21: SBF tests of unetched hydroxyapatite coated and hydroxyapatite/chitosan coated substrates. Etched HAp coated(left) HAp-Chitosancoated(right).

Samples kept in SBF are shown in the images above. The change in the sample coated with chitosan in petri flask number 4 proved the bioactivity. The whitening of the formed apatite layer confirmed this result.

10. CONCLUSION

Within the scope of this thesis, a 4-step production was made with the inclusion of test phase. On the basis of these steps, a bone-like bioceramic was produced and an increased bioactivity was aimed at its surface. In the production phase, tape casting technology was used and a 4-layer functionally graded silicon nitride structure was produced. This process is very useful for obtaining functionally graded bone-like structures in the most cost-efficient way. Lamination was made by increasing the amount of porous agent in the prepared suspensions and a variable porous structure was obtained after the binder removal process. It has been proven that a bone-like structure is obtained from the obtained SEM images.

Since the porosity observed in the structure was thought to have positive effects on the adhesion of the coatings, some of the samples were etched. Since a homogeneous etching is desired during the etching processes, etching was done with the reverse flow method and the samples were prepared for the coating processes.

In the coating process, dip coating method was chosen in order to synthesize water-based hydroxyapatite. It was predicted that both coating and doping effect would be created on the high porosity structure and these results were obtained. It is known from other studies that the presence of only hydroxyapatite in the structure increases the bioactivity, but its production on the surface in the form of synthesis has not been encountered before. In this context, it was known that the activity effect would be obtained with hydroxyapatite. This is a very difficult process to increase bioactivity and perform on functionally graded silicon nitride.

In this context, chitosan coating, which is in perfect harmony with hydroxyapatite and is known to increase bioactivity in different materials, has been considered and applied. After the coating processes, SBF was used for the bioactivity measurements of the materials and the activity was interpreted by keeping it waiting for certain periods. As seen in the other chapters, a very intense increase in bioactivity was observed in the samples where chitosan and hydroxyapatite were coated together, within the duration of storage in SBF and in the light of SEM images.

As a result of the tests, it was concluded that the thesis was successful. Functionally graded silicon nitride material coated with Chitosan and Hydroxyapatite has been achieved to obtain a higher bioactivity compared to previous studies. It has

been proven that it is possible to try different coating types or try different coating components, and possible studies have been opened.



REFERENCES

- Abbott N.J., Lannefeld T., Barish L., Brysson R., (1972), "Study of tearing in coated cotton fabrics- 3." *J Coated Fibrous Mater*, 1(1971), 130–149.
- Alonso S., Bertrand F., Tanguy P.A., (2003), "A torque-based analysis of the reverse roll coating process." *Chemical Engineering Science*, 58(9), 1831–1837.
- Asri R. I. M., Harun W. S. W., Hassan M. A., Ghani S. A. C., Buyong Z., (2016), "A review of hydroxyapatite-based coating techniques: Sol-gel and electrochemical depositions on biocompatible metals." *Journal of the Mechanical Behavior of Biomedical Materials*, 57, 95–108.
- Aurobind S. V., Amirthalingam K. P., Gomathi H., (2006), "Sol-gel based surface modification of electrodes for electro analysis." *Advances in Colloid and Interface Science*, 121(1–3), 1–7.
- Ayas E., (2009), "Si₃N₄ Esaslı Kompozit Malzemelerin Elektriksel ve Isıl İletkenliklerinin Geliştirilmesi." PhD Thesis, July. Anadolu Üniversitesi.
- Bal B. S., Garino J., Ries M., Rahaman M. N., (2006). "Ceramic Materials in Total Joint Arthroplasty." *Seminars in Arthroplasty JSES*, 17(3–4), 94–101.
- Bezzi G., Celotti G., Landi E., La Torretta, T. M. G. Sopyan I., Tampieri A., (2003), "A novel sol-gel technique for hydroxyapatite preparation." *Materials Chemistry and Physics*, 78(3), 816–824.
- Borello A., Deptuła A., Łada W., Olczak T., Alvani C., Di Bartolomeo A., (1992), "Non-Crystalline Solids Preparation of spherical powders of hydroxyapatite." *Journal of Non-Crystalline Solids*, 148, 537–541.
- Bressiani J. C., Izhevskiy V., Bressiani A. H., (1999). "Development of the Microstructure of the Silicon Nitride Based Ceramics 2 . Factors Governing Microstructure Formation in Si₃N₄ -based Ceramics 3 . Models of Exaggerated Grain Growth in Si₃N₄-based Ceramics and Model." *Development*, 2(3), 165–172.
- Brown P. W., Constantz B., (1994), "Hydroxyapatite" Editors. 148-153
- Butts D. I., LaCourse W. C., Kim S., (1988), "Influence of sol and substrate chemistry on the formation of sol-gel derived coatings." *Journal of Non-Crystalline Solids*, 100(1–3), 514–518.
- Buyuksagis I. S., Uygunoglu T., Tatar E., (2017), "Investigation on the usage of waste marble powder in cement-based adhesive mortar." *Construction and Building Materials*, 154, 734–742.
- Carrado A., Pelletier H., Rol T., (2011), "Nanocrystalline Thin Ceramic Films Synthesised by Pulsed Laser Deposition and Magnetron Sputtering on Metal

Substrates for Medical Applications." *Biomedical Engineering - From Theory to Applications*, 202-214.

Chai C. S., Ben-Nissan B., (1999), "Bioactive nanocrystalline sol-gel hydroxyapatite coatings." *Journal of Materials Science: Materials in Medicine*, 10(8), 465–469.

Davies I. J., (2017), "Mechanical properties of silicon carbide composites fabricated with short inorganic fibers." *April. Development*, 2(3), 185–190.

Du M., Chen J., Liu K., Xing H., Song C., (2021), "Recent advances in biomedical engineering of nano-hydroxyapatite including dentistry, cancer treatment and bone repair." *Composites Part B: Engineering*, 215(February), 122-143.

Ducheyne P., Hastings G. W., (2018), "Metal and Ceramic Biomaterials." In *Metal and Ceramic Biomaterials*. 2(3), 165–172.

Dutta P. K., Ravikumar M. N. V., Dutta J., (2002), Chitin and chitosan for versatile applications. *Journal of Macromolecular Science - Polymer Reviews*, 42(3), 307–354.

Dwivedi R., Zekovic S., Kovacevic R., (2006), Field feature detection and morphing-based process planning for fabrication of geometries and composition control for functionally graded materials. *Proceedings of the Institution of Mechanical Engineers, Part B: Journal of Engineering Manufacture*, 220(10), 1647–1661.

Elliott J. C., Mackie P. E., Young R. A., (1973), "Monoclinic hydroxyapatite." *Science*, 180(4090), 1055–1057.

Feng B., Weng J., Yang B. C., Qu S. X., Zhang X. D., (2003), "Characterization of surface oxide films on titanium and adhesion of osteoblast." *Biomaterials*, 24(25), 4663–4670.

Fernandes J. S., Gentile P., Pires R. A., Reis R. L., Hatton P. V., (2017), "Multifunctional bioactive glass and glass-ceramic biomaterials with antibacterial properties for repair and regeneration of bone tissue." *Acta Biomaterialia*, 59, 2–11.

Ferraz M. P., Monteiro F. J., Manuel C. M., (2004), "Hydroxyapatite nanoparticles: A review of preparation methodologies." *Journal of Applied Biomaterials & Biomechanics : JABB*, 2(2), 74–80.

García-Godoy F., Hicks M. J., (2008), "Maintaining the integrity of the enamel surface: The role of dental biofilm, saliva and preventive agents in enamel demineralization and remineralization." *Journal of the American Dental Association*, 139, 25-34.

Glawe A., Reuscher R., Köppe R., Kolbusch T., (2003), "Hot-melt application for functional compounds on technical textiles." *Journal of Industrial Textiles*, 33(2), 85–92.

Greer R., (1995), "The Reverse Roll Coater." *Journal of Coated Fabrics*, 24(4), 287–297.

Gupta K. C., Ravi Kumar M. N. V., (2000), "Overview on chitin and chitosan applications with an emphasis on controlled drug release formulations." *Journal of Macromolecular Science - Reviews in Macromolecular Chemistry and Physics*, 40-55.

Gupta R., Chaudhury N. K., (2007), "Entrapment of biomolecules in sol-gel matrix for applications in biosensors: Problems and future prospects." *Biosensors and Bioelectronics*, 22(11), 2387–2399.

Hampshire S., (2016), "Silicon Nitride Ceramics." *Engineered Ceramics: Current Status and Future Prospects*, 102, 77–97.

Heimann R. B., (2010), "Classic and Advanced Ceramics: From Fundamentals to Applications." *Classic and Advanced Ceramics: From Fundamentals to Applications* 14(12),

Heimann R. B., (2021), "Silicon Nitride, a Close to Ideal Ceramic Material for Medical Application." *Ceramics*, 4(2), 208–223.

Hing K. A., Best S. M., Bonfield W., (1999), "Characterization of porous hydroxyapatite." *Journal of Materials Science: Materials in Medicine*, 10(3), 135–145.

Hirano S., Ohe Y., Ono H., (1976), "Selective N-acylation of chitosan." *Carbohydrate Research*, 47(2), 315–320.

Hulbert S. F., Hench L. L., Forbers D., Bowman L. S., (1982), "History of bioceramics." *Ceramics International*, 8(4), 131–140.

Itokazu M., Yang W., Aoki T., Ohara A., Kato N., (1998), "Synthesis of antibiotic-loaded interporous hydroxyapatite blocks by vacuum method and in vitro drug release testing." *Biomaterials*, 19(7–9), 817–819.

Jansen M., (2002), "High Performance Non-Oxide Ceramics II." Springer Vienna.

Ji G., Zhao M., (2017), "Membrane Separation Technology in Carbon Capture." *Recent Advances in Carbon Capture and Storage*.

Jiang Q., Tong H. Y., Hsu D. T., Okuyama K., Shi F. G., (1998), "Thermal stability of crystalline thin films." *Thin Solid Films*, 312(1–2), 357–361.

Kayali E. S., El-Sayed M., Funke P., (1990), "Deformation behaviour during drawing of copper rods produced using various processes." *Materials Science and Technology (United Kingdom)*, 6(9), 872–882.

Kloskowski A., Pilarczyk M., Chrzanowski W., Namieśnik J., (2010), "Sol-gel technique-a versatile tool for adsorbent preparation." *Critical Reviews in Analytical Chemistry*, 40(3), 172–186.

Kokubo T., Takadama H., (2006), "How useful is SBF in predicting in vivo bone bioactivity?" *Biomaterials*, 27(15), 2907–2915.

Kokubo T., Takadama H., (2008), "Simulated Body Fluid (SBF) as a Standard Tool to Test the Bioactivity of Implants." *Handbook of Biomineralization: Biological Aspects and Structure Formation*, 3, 97–109.

Kokubo T., Yamaguchi S., (2019), "Simulated body fluid and the novel bioactive materials derived from it." *Journal of Biomedical Materials Research - Part A*, 107(5), 968–977.

Koshino T., Okamoto R., Takagi T., Yamamoto K., Saito T., (2002), "Cemented ceramic YMCK total knee arthroplasty in patients with severe rheumatoid arthritis." *Journal of Arthroplasty*, 17(8), 1009–1015.

Krämer M., Hoffmann M. J., Petzow G., (1993), "Grain growth kinetics of Si₃N₄ during α/β -transformation." *Acta Metallurgica Et Materialia*, 41(10), 2939–2947.

Lacefield W. R., (1988), "Hydroxyapatite Coatings." *Annals of the New York Academy of Sciences*, 523(1), 72–80.

LeGeros R. Z., (1988), "Calcium phosphate materials in restorative dentistry: a review." *Advances in Dental Research*, 2(1), 164–180.

Lewis, P. M., Al-Belooshi A., Olsen M., Schemitch E. H., Waddell J. P., (2010), "Prospective randomized trial comparing alumina ceramic-on-ceramic with ceramic-on-conventional polyethylene bearings in total hip arthroplasty." *Journal of Arthroplasty*, 25(3), 392–397.

Liu D. M., Troczynski T., Tseng W. J., (2001), "Water-based sol-gel synthesis of hydroxyapatite: Process development." *Biomaterials*, 22(13), 1721–1730.

Livage J., Beteille F., Roux C., Chatry M., Davidson P., (1998), "Sol-gel synthesis of oxide materials." *Acta Materialia*, 46(3), 743–750.

Livage J., Ganguli D., (2001), "Sol-gel electrochromic coatings and devices: A review." *Solar Energy Materials and Solar Cells*, 68(3–4), 365–381.

Locher M., Romano V., Weber H. P., (2005), "Rare-earth doped sol-gel materials for optical waveguides." *Optics and Lasers in Engineering*, 43(3–5),

Makhlouf A. S. H., (2011), "Current and advanced coating technologies for industrial applications." *Nanocoatings and Ultra-Thin Films*. 55(5). Woodhead Publishing Limited.

Mazzocchi M., Bellosi A., (2008), "On the possibility of silicon nitride as a ceramic for structural orthopaedic implants. Part I: Processing, microstructure, mechanical properties, cytotoxicity." *Journal of Materials Science: Materials in Medicine*, 19(8), 2881–2887.

Mobasherpour I., Heshajin M. S., Kazemzadeh A., Zakeri M., (2007), "Synthesis of nanocrystalline hydroxyapatite by using precipitation method." *Journal of Alloys and*

Compounds, 430(1–2), 330–333.

Montenero A., Gnappi G., Ferrari F., Cesari M., Salvioli E., (2000), "Sol-gel derived hydroxyapatite coatings." *Journal of Materials Science*, 5, 2791–2797.

Moore G. K., Roberts G. A. F., (1981), "Reactions of chitosan: 2. Preparation and reactivity of N-acyl derivatives of chitosan." *International Journal of Biological Macromolecules*, 3(5), 292–296.

Mori A., (1992), "A histological study of the augmented reconstruction of the anterior cruciate ligament in rabbits." *Nippon Ika Daigaku Zasshi*, 59(2), 176–185.

Mourya V. K., Inamdar N. N., (2008), "Chitosan-modifications and applications: Opportunities galore." *Reactive and Functional Polymers*, 68(6), 1013–1051.

Naik K. S., (2019), "Advanced bioceramics." *Advances in Biological Science Research: A Practical Approach*. 43(2). Elsevier Inc.

Nishimura S. I., Kohgo O., Kurita K., Kuzuhara H., (1991), "Chemospecific Manipulations of a Rigid Polysaccharide: Syntheses of Novel Chitosan Derivatives with Excellent Solubility in Common Organic Solvents by Regioselective Chemical Modifications." *Macromolecules*, 24(17), 4745–4748.

Orman Z., (2017), "Bioactivity Test and Cell Studies of Bioceramics Produced from *Clinocardium Ciliatum* and *Turritella Terebra*." Master's Thesis. Yildiz Technical University.

Osaka A., Miura Y., Takeuchi K., Asada M., Takahashi K., (1991), "Calcium apatite prepared from calcium hydroxide and orthophosphoric acid." *Journal of Materials Science: Materials in Medicine*, 2(1), 51–55.

Owens G. J., Singh R. K., Foroutan F., Alqaysi M., Han C. M., Mahapatra C., Kim H. W., Knowles J. C. (2016), "Sol-gel based materials for biomedical applications." *Progress in Materials Science*, 77, 1–79.

Allen P.C., (1998), "Introduction to Sol-Gel Processing The International Series in Sol-Gel Processing: Technology & Applications." (66) 3. Kluwer Academic Publisher.

Pillar-Little E. A., Zhou R., Guzman M. I., (2015), Heterogeneous Oxidation of Catechol. *Journal of Physical Chemistry A*, 119(41), 10349–10359.

Rao Arathi., Neeraj M., (2013), "The role of remineralizing agents in dentistry: A review." *Compendium*, April, 25–34.

Rujitanapanich S., Kumpapan P., Wanjanoi P., (2014), "Synthesis of hydroxyapatite from oyster shell via precipitation." *Energy Procedia*, 56(C), 112–117.

Salosarczyk A., Stobierska E., Paszkiewicz Z., Gawlicki M., (2005), "Calcium Phosphate Materials Prepared from Precipitates with Various Calcium:Phosphorus Molar Ratios." *Journal of American Ceramic Society*, 79(10), 2539–2544.

Shanmugam K., Sahadevan R., (2018), "Bioceramics-An introductory overview." Fundamental Biomaterials: Ceramics. Elsevier Ltd.

Shih W. J., Chen Y. F., Wang M. C., Hon M. H., (2004), "Crystal growth and morphology of the nano-sized hydroxyapatite powders synthesized from $\text{CaHPO}_4 \cdot 2\text{H}_2\text{O}$ and CaCO_3 by hydrolysis method." Journal of Crystal Growth, 270(1–2), 211–218.

Shim E., (2013), "Bonding requirements in coating and laminating of textiles." Joining Textiles: Principles and Applications. 72, 62–79.

Sobolev E. V., Lisoivan V. I., (1969), "Nitrogen in the lamellar defects of diamond." In Journal of Structural Chemistry (Vol. 10, Issue 4). 510-530.

Somiya S., Mitomo M., Yoshimura M., (1991), "Silicon Nitride - I Ceramic Research and Development in Japan, Vol. 1." Materials and Manufacturing Processes, 6(4), 741–744.

Sopyan I., Singh R., Hamdi M., (2008), "Synthesis of nano sized hydroxyapatite powder using sol-gel technique and its conversion to dense and porous bodies." Indian Journal of Chemistry - Section A Inorganic, Physical, Theoretical and Analytical Chemistry, 47(11), 1626–1631.

Stankevičiute Ž., Malakauskaite M., Beganskiene A., Kareiva A., (2013), "Sol-gel synthesis of calcium phosphate coatings on Ti substrate using dip-coating technique." Chemija, 24(4), 288–295.

Supancic P., Danze R., Harrer W., Wang Z., Witschnig S., Schöppl O., (2009), "Strength tests on silicon nitride balls." Key Engineering Materials, 409, 193–200.

Tsukamoto R., Chen S., Asano T., Ogino M., Shoji H., Nakamura T., Clarke I., (2006), "Improved wear performance with crosslinked UHMWPE and zirconia implants in knee simulation." Acta Orthopaedica, 77(3), 505–511.

Uchida M., Kim H. M., Kokubo T., Fujibayashi S., Nakamura T., (2003), "Structural dependence of apatite formation on titania gels in a simulated body fluid." Journal of Biomedical Materials Research - Part A, 64(1), 164–170.

Wei P., Chen L., Okubo A., Hirai T., (2001), "Tough multilayered α - β Si_3N_4 ceramics prepared by spark plasma sintering." Materials Letters, 49(3–4), 239–243.

Wright V. P., (1994). "Paleosols in shallow marine carbonate sequences." Earth Science Reviews, 35(4), 367–395.

Yoshimura M., Suda H., Okamoto K., Ioku K., (1994), "Hydrothermal synthesis of biocompatible whiskers." Journal of Materials Science, 29(13), 3399–3402.

Young R. A., Holcomb D. W., (1982), "Variability of hydroxyapatite preparations." Calcified Tissue International, 34 Suppl 2, S17–32.

Zhang X., (2007), "Preparation and Characterization of Calcium Phosphate Ceramics and Composites as Bone Substitutes." PhD Thesis. University of California , San Diego.



BIOGRAPHY

Ertançan BABAÇ is Graduated from Burhan Felek Anatolian High School. Started and achieve his bachelor degree from Sakarya University, Metallurgical and Materials Engineering. Then started his master's degree at Gebze Technical University Material Science and Engineering. Completed his Master's Thesis at TUBITAK-MRC Materials Institute under an international project between TUBITAK-MRC&SAS (Slovakia Academy of Science).

